Gondwana Research 24 (2013) 90–103

Contents lists available at SciVerse ScienceDirect

Gondwana Research

journal homepage: www.elsevier.com/locate/gr

GR focus review

Permian and Triassic greenhouse crises

Gregory J. Retallack *

Department of Geological Sciences, University of Oregon, Eugene, OR 97403, United States

ARTICLE INFO

Article history:
Received 11 January 2012
Received in revised form 8 March 2012
Accepted 9 March 2012
Available online 23 March 2012

Keywords:
Paleosol
Carbon dioxide
Greenhouse
Paleoclimate
Permian
Triassic

ABSTRACT

Paleoclimatic time series from Permian and Triassic paleosols reveal transient episodes of unusually warm and wet conditions, interrupting long periods of cool and dry conditions usual for calcareous red paleosols. Some of these paleoclimatic events are known from stomatal index of fossil *Lepidopteris* leaves to have been episodes of elevated global atmospheric CO_2. The magnitude of 19 known Permian and Triassic greenhouse crises varied considerably, and they offer new evidence for the relationship between paleoclimate and atmospheric CO_2 levels. These greenhouse crises also had marked effects on global lowland vegetation, introducing frost-sensitive tropical lycopsids to high latitudes and drought-tolerant conifers to low latitude lowlands. Greenhouse events punctuate phases in plant evolution (*Ottokaria–Callipteris*, *Plumsteadia–Rufloria*, *Lidgettonia–Tatarina*, *Pleuromeia*, and *Dicroidium–Scytophyllum* floras). Greenhouse events also punctuate the evolution of reptilian dynasties (successive pelycosaur, dinocephalian, dicynodont, rhynchosaur and dinosaur faunas) and respiratory adaptations (such as enlarged bony secondary palate). Greenhouse crises of the Late and Middle Permian were the most severe known, and suggest a role for atmospheric pollution with CH_4 and CO_2 in those mass extinction events, probably from thermogenic cracking of coals by intrusive feeder dikes of flood basalts. Because of formalities in boundary definition these mass extinctions are neither "end-Permian" nor "end-Guadalupian", but upper Changhsingian and mid-Capitanian, respectively.

Contents

1. Introduction

By the year 2100, atmospheric CO_2 partial pressures are predicted to triple, from pre-industrial levels of 280 ppm to some 856 ppm (+70/−101 ppm: using emission scenario A2, very heterogeneous world with continued population growth of Solomon et al., 2007). Such changes are unprecedented in Quaternary records (Lüthi et al., 2008), and are best tested by proxies for atmospheric CO_2 deeper in geological time (Royer, 2006). The Permian and Triassic periods offer an array of greenhouse crises (Retallack, 2005a, 2009a), including the largest known Phanerozoic CO_2 levels coincident with the largest known Phanerozoic mass extinction (Retallack and Jahren, 2008). Furthermore, high resolution sequences of paleosols now show that many Permian and Triassic greenhouse crises were geologically abrupt transients (Retallack, 2009a), in some cases on time scales comparable with the current greenhouse crisis driven by fossil fuel consumption (Solomon et al., 2007). Lacustrine deposits yield fossil leaf stomatal index evidence for Early Triassic CO_2 plummeting from 3860 to 305,

* Tel.: +1 541 346 4558; fax: +1 541 346 4692.
E-mail address: gregr@uoregon.edu.

1342-937X/$ – see front matter
doi:10.1016/j.gr.2012.03.003

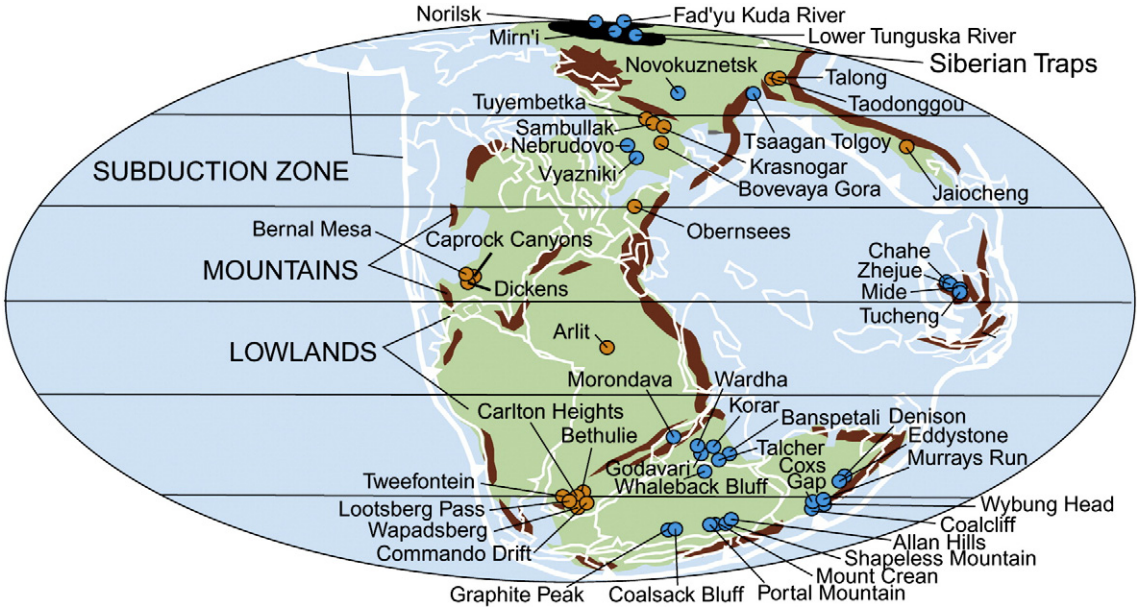

Fig. 1. Late Permian map of the world showing non-marine Permian–Triassic boundary sections of calcareous red beds (Table 1) and of coal measures (Table 2). Marine boundary sections are too numerous to be depicted at this map scale (91 sites are listed by Korte and Kozur, 2010).

then 417 and 3510 ppm, all within only 130,000 years (Retallack et al., 2011). Isotopic proxies for Late Permian atmospheric methane reveal dramatic fluctuations (−5‰ $\delta^{13}C_{org}$) within as few as 800 annual varves (Retallack and Jahren, 2008). Permian–Triassic greenhouse crises were abrupt and often brutal. Gases such as methane from thermogenic cracking of coal by large intrusive precursors to Siberian trap lavas have been suggested as causes of these Late Permian and Early Triassic greenhouse crises (Retallack and Jahren, 2008; Grasby et al., 2011). Also likely were massive volcanic emissions of HCl (Sobolev et al., 2011) and Hg (Sanei et al., 2012). Other kill mechanisms include degassing of H_2S, CH_4 or CO_2 from an anoxic and acidified ocean (Grice et al., 2005; Kump et al., 2005; Şengör and Atayman, 2009), release of marine and permafrost methane clathrate or gas (Heydari and Hassandzadeh, 2003; Ryskin, 2003), or impact of large asteroids or comets (Becker et al., 2001, 2004). Such events were not restricted to the Late Permian and Early Triassic: Emeishan flood basalts may coincide with mid-Capitanian mass extinction (Retallack and Jahren, 2008; Retallack et al., 2011) and Wrangellia flood basalts may coincide with early Carnian biotic overturn (Dal Corso et al., 2012).

This review concerns not such theories (ably reviewed by Korte et al., 2010), but rather empirical evidence for timing and duration of Permian and Triassic CO_2 greenhouses from non-marine rock sequences (Fig. 1), primarily paleosols of calcareous red beds (Table 1) and peaty wetlands (Table 2). The marine record of atmospheric CO_2 and paleoclimate is muted and imprecise (Rothman, 2002; Berner, 2006), and has been reviewed elsewhere (Korte and Kozur, 2010). Much work on the Permian–Triassic boundary has focused on coal measure sequences with well-preserved fossil pollen and leaves (Kazarinova, 1979; Wright and Askin, 1987; Sadovnikov and Orlova, 1990; Retallack, 1995, 1999; Morante, 1996; Wang, 1996; Krull and Retallack, 2000; de Wit et al., 2002; Sarkar et al., 2003; Retallack et al., 2005, 2006, 2007; Lindström and McLoughlin, 2007; Johnson et al., 2008; Sadovnikov, 2008, 2011; Krassilov and Karasev, 2009; Mogutcheva and Krugovykh, 2009; Davies et al., 2010; Mogutcheva and Naugolnykh, 2010). This paper instead emphasizes ongoing studies of calcareous red beds (Retallack et al., 2003; Retallack, 2005a; Coney et al., 2007; Szurlies, 2007; Taylor et al., 2009; Inosemtsev and Targulian, 2010; Tabor et al., 2011; Thomas et al., 2011; Benton et al., 2012; Newell et al., 2012), with their distinctive aridland paleosols (Aridosols, Alfisols, and Vertisols) and fossil vertebrates (Figs. 2–3). There have been difficulties understanding the Permian–Triassic transition in calcareous red beds because plant fossils are rare to lacking (Gastaldo et al., 2005), and

Table 1
Calcareous red bed Permian–Triassic boundary sections.

Locality	GPS position	Permian formations	Triassic formations	References
Arlit, Niger	N7.251954 E17.717555	Moradi Formation	Telqua Formation	Tabor et al., 2011
Bernal Mesa, New Mexico, USA	N35.39339 W105.29997	Bernal Fm.	Anton Chico Fm.	Retallack, 2005a
Bethulie, South Africa	S30.415899 E26.262209	Balfour Fm.	Katberg Sandstone	Retallack et al., 2003
Bovevaya Gora, Russia	N51.304616 E54.907964	Kulchumovskaya	Kopanskaya Svita	Taylor et al., 2009
Cap Rock Canyons, Texas, USA	N34.45346 W101.081580	Alibates Fm.	Dewey Lake Fm.	Retallack, 2005a
Carlton Heights, South Africa	S31.295033 E24.915155	Balfour Fm.	Katberg Sandstone	Retallack et al., 2003
Commando Drift, South Africa	S32.169550 E26.0533317	Balfour Fm.	Katberg Sandstone	Coney et al., 2007
Dickens, Texas, USA	N33.62552 W100.81791	Alibates Fm.	Dewey Lake Fm.	Retallack, 2005a
Lootsberg Pass, South Africa	S31.852132 E24.873138	Balfour Fm.	Katberg Sandstone	Retallack et al., 2003
Obernsees, Germany	N49.914927 E11.374448	Bröckelschiefer	Geinhausen Fm.	Szurlies, 2007
Sambullak, Russia	N51.877001 E56.207016	Kulchumovskaya	Kopanskaya Svita	Taylor et al., 2009
Taodonggou, NW China	N43.260342 E88.978817	Guodeking Fm.	Jiucaiyuan Fm.	Thomas et al., 2011
Tarlong, NW China	N43.263978 E89.036817	Guodeking Fm.	Jiucaiyuan Fm.	Thomas et al., 2011
Tuyembetka, Russia	N51.918510 E56.337648	Kulchumovskaya	Kopanskaya Svita	Taylor et al., 2009
Tweefontein, South Africa	S31.798666 E24.79219	Balfour Fm.	Katberg Sandstone	Ward et al., 2005
Wapadsberg, South Africa	S31.923139 E24.923139	Balfour Fm.	Katberg Sandstone	Ward et al., 2005

Table 2
Coal measure Permian–Triassic boundary sections.

Locality	GPS position	Permian formations	Triassic formations	References
Allan Hills, Antarctica	S76.70240 E159.73623	Weller C.M.	Feather Congl.	Retallack et al., 2005
Banspetali (Raniganj), India	N23.617511 E86.895819	Raniganj Fm.	Panchet Fm.	Sarkar et al., 2003
Chahe, Guizhou, China	N26.688496 E103.778506	Kayitou Fm.	Dongchuan Fm.	Shen et al., 2011
Chuanyan, Sichuan, China	N28.169361 E105.082111	Wangjiazhai Fm.	Feixuanguan Fm.	Shen et al., 2011
Coalcliff, NSW, Australia	S34.256251 E150.973237	Eckersley Fm.	Coal Cliff Ss.	Retallack, 1999
Coalsack Bluff, Antarctica	S84.23898 E162.29979	Buckley C.M.	Fremouw Fm.	Retallack et al., 2005
Coxs Gap. NSW, Australia	S32.435836 E150.207014	Farmers Ck Fm.	Widdin Brook	Retallack, 1999
Denison bore, Qld, Australia	S23.749425 E147.89658	Rangal Coal M.	Rewan Fm.	Morante, 1996
Eddystone 1, Qld, Australia	S24.955465 E148.518282	Rangal Coal M.	Rewan Fm.	Morante, 1996
Fad'yu Kuda River, Siberia	N74.083645 E97.650238	Zverinskaya Sv.	Betlinskaya Sv.	Sadovnikov and Orlova, 1990
Godavari Coalfield, India	N17.964679 E80.759085	Raniganj Fm.	Panchet Fm.	de Wit et al., 2002
Graphite Peak, Antarctica	S85.05211 E172.36832	Buckley C.M.	Fremouw Fm.	Retallack et al., 2005
Jiaocheng, North China	N37.569273 E112.122137	Sunjiagiou Fm.	Liujiagou Fm.	Wang, 1996
Korar Coalfield, India	N23.181065 E82.337245	Raniganj Fm.	Panchet Fm.	de Wit et al., 2002
Gagarii Island, Siberia	N63.772339 E97.510260	Bugariktinskaya	Nidimskaya Sv.	Kozur and Weems, 2011
Guanbachong, Yunnan, China	N27.404333 E103.56325	Xuanwei Fm.	Dongchuan Fm.	Shen et al., 2011
Longmendong, Sichuan, China	N29.584556 E103.41533	Xuanwei Fm.	Dongchuan Fm.	Shen et al., 2011
Mide, Yunnan, China	N26.236943 E104.596324	Kayitou Fm.	Dongchuan Fm.	Shen et al., 2011
Mirn'i, Siberia	N61.996139 E113.861321	Bugarikta Svita	Ukugutskoi S.	Kazarinova, 1979
Morondava, Madagascar	S21.359622 E45.506862	Lower Sakamena	Mid-Sakamena	Wright and Askin, 1987
Mount Crean, Antarctica	S77.87383 E159.53333	Weller C.M.	Feather Congl.	Retallack et al., 2005
Murrays Run bore, Australia	S33.071585 E151.15253	Redmanville Ck.	Dooralong Sh.	Retallack, 1999
Nebrudovo, Russia	N60.149611 E45.816111	Vyaznikovian	Nebrudovian	Krassilov and Karasev, 2009
Noril'sk, Siberia	N69.37439 E88.127041	Nadezhdinskaya	Mokulaevskaya	Sadovnikov and Orlova, 1990
Novokutznetsk, Siberia	N54.388827 E87.534582	Yerunakovskaya	Mal'tsevskaya	Davies et al., 2010
Portal Mountain, Antarctica	S78.10784 E159.36727	Weller C.M.	Feather Congl.	Retallack et al., 2006
Shapeless Mountain, Antarctica	S77.43797 E160.47073	Weller C.M.	Feather Congl.	Retallack et al., 2005
Talcher Basin, India	N20.960523 E85.123355	Raniganj Fm.	Panchet Fm.	de Wit et al., 2002
Tsaagan Tolgoy, Mongolia	N42.560157 E105.361833	Tsaagan Tolgoy	Tavan Tolgoy	Johnson et al., 2008
Tucheng, Guizhou, China	N25.654341 E104.371393	Kayitou Fm.	Dongchuan Fm.	Shen et al., 2011
Vyazniki, Russia	N56.318194 E42.138806	Vyaznikovian	Nebrudovian	Krassilov and Karasev, 2009
Wardha Coalfield, India	N20.052258 E79.305261	Raniganj Fm.	Panchet Fm.	de Wit et al., 2002
Whaleback Bluff, Antarctica	S70.528349 E68.257439	Bainmedart C.M.	Flagstone Bench	Lindström and McLoughlin, 2007
Wybung Head, NSW, Australia	S33.197483 E151.621853	Karignan Congl.	Dooralong Sh.	Retallack, 1999
Zhongzhai, Guizhou, China	N26.156435 E105.287076	Wangjiazhai Fm.	Feixuanguan Fm.	Shen et al., 2011

vertebrate fossils are sporadic in occurrence (Benton et al., 2004; Ward et al., 2005; Gastaldo et al., 2009). Fortunately, paleosols provide a remarkably complete record of Permian and Triassic climate and vegetation that can be used to supplement paleontological records (Retallack et al., 2003; Retallack, 2005a; Thomas et al., 2007, 2011; Taylor et al., 2009). Unlike paleosols of coal measures which were partially or entirely waterlogged as they sank below thick peats and were isolated from the atmosphere, formerly well drained paleosols of calcareous red beds formed over substantial periods of time (millennia) in full contact with the atmosphere and biosphere (Retallack, 1997a, 2001). These paleosols are massive and hackly from the activity of roots and burrows disrupting original bedding of sedimentary parent materials, and have a horizon of calcareous nodules below surface rooted horizons (Figs. 2b, d, and 3b, d). These modified beds punctuate long sequences of alluvial and aridland sedimentary deposits (Figs. 2a, c, and 3a, c). Many features of such red calcareous paleosols can be used as quantitative proxies for past CO_2 and a variety of paleoclimatic parameters (Retallack, 2005a, 2009b; Sheldon and Tabor, 2009), as reviewed here. Furthermore, these greenhouse crises had marked effects on animals and plants and their fossil record of the Permian and Triassic, as also reviewed here.

2. Materials and methods

Many paleosol sequences are now known in Permian and Triassic calcareous red beds (Table 1) and coal measures (Table 2). Calcareous red paleosols of the Karoo Basin of South Africa (Fig. 2a–b: Retallack et al., 2003; Ward et al., 2005), Cis-Uralian Russia (Fig. 2c–d: Benton et al., 2004; Inosemtsev and Targulian, 2010) and Niger (Tabor et al., 2011) are known for their fossil vertebrates. More revealing sequences, because of the abundance of paleosols, have now been found in Texas–Oklahoma (Fig. 3c–d) and Utah–New Mexico (Fig. 3a–b). Utah–New Mexico has a composite sequence of paleosols ranging from the base of the Permian to the top of the Triassic (Retallack, 2009a), which can be used as a paleoclimatic standard until other records are comparably documented. Because of the data-density of paleosols in the red rock country of Utah and New Mexico, this region reveals the transient and non-periodic nature, and varied magnitude, of paleoclimatic events. These events were defined (by Retallack, 2009a) as proxies more than 2 standard deviations beyond a 10-point running mean value. Many of the paleoclimatic excursions were short-lived events (100,000 years or less) and they were separated in time by millions to tens of millions of years. Of the 19 Permian and Triassic paleoclimatic events, 5 were clustered within the 4.4-million-year span of the Early Triassic (time scale revised from Gradstein et al., 2004, by Ovtcharova et al., 2006; Shen et al., 2011).

Identification of paleoclimatic excursions requires close attention to meter level of each paleosol within stratigraphic sections. Paleosols are ubiquitous in red beds that have already been studied for radiometric dating of ashes, or paleomagnetic stratigraphy. With meter levels of geochronological tie points the relative age of each paleosol can then be inferred by linear regression of meter level versus geological age in local sections (Retallack, 2005a, 2009a). Abrupt climate shifts are also apparent from paleoclimatic proxies plotted by meter level (Tabor et al., 2002; Tabor and Montañez, 2004; Tabor, 2007). Such transients cannot be detected in time series lumping paleoclimatic proxy data by formations (Ekart et al., 1999; Montañez et al., 2007), by biostratigraphic zones (Angielczyk and Walsh, 2008), or within 10 million year or longer bins (Rothman, 2002; Berner, 2006). Such data smoothing lacks stratigraphic resolution required to identify transient paleoclimatic excursions.

Thousands of Permian and Triassic paleosols have now been documented, but most are known only from reconnaissance studies. Detailed description and naming of particular kinds of paleosols, or

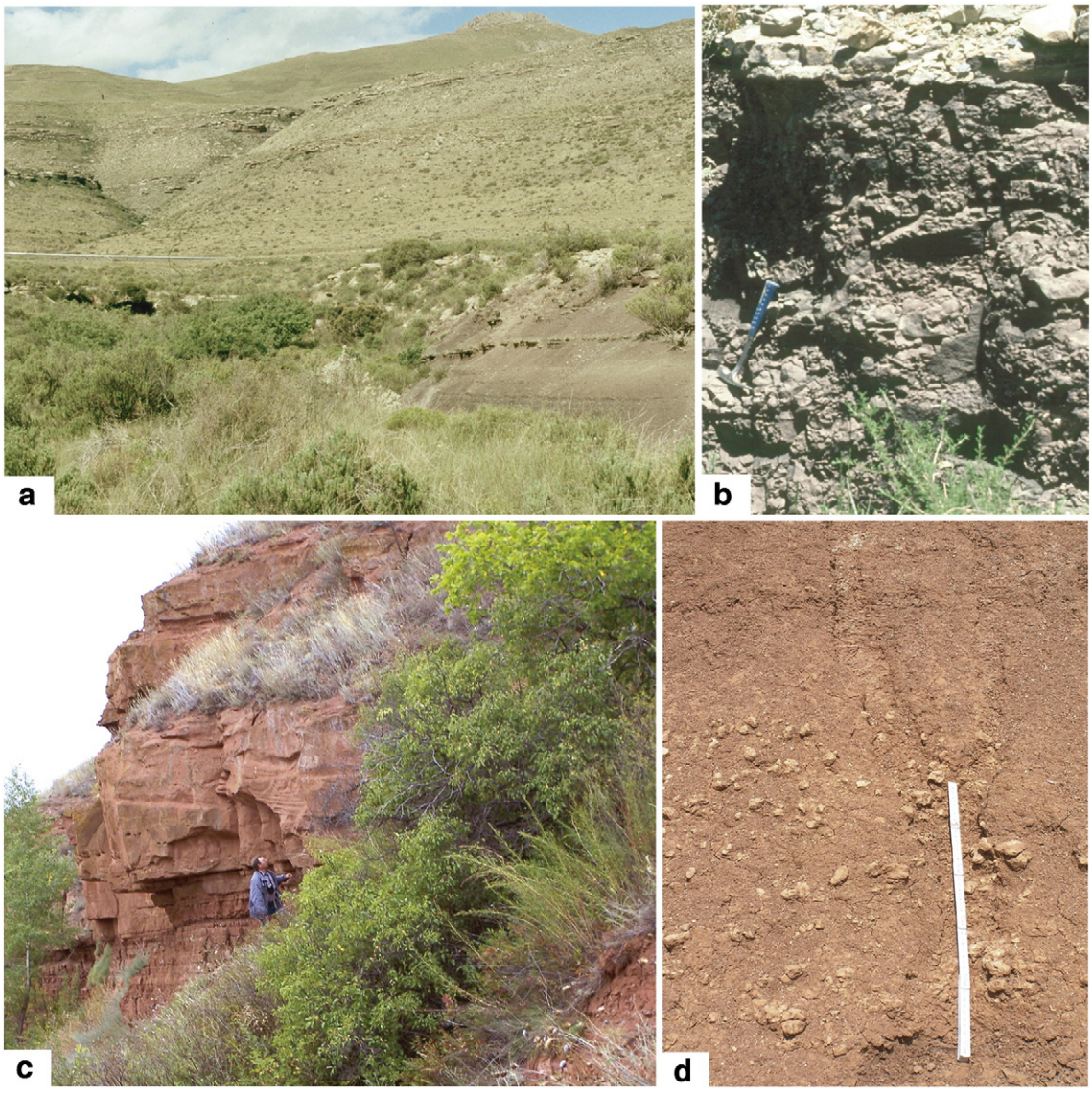

Fig. 2. Calcareous red bed sections of the Karoo Basin, South Africa (a–b) and Cis-Uralian Russia (c–d). (a) Laminites of upper Palingkloof Member of Balfour Formation (0 to −5 m in section of Retallack et al., 2003), with sandstones of Katberg Formation in hills behind at Lootsberg Pass. (b) Karie pedotype paleosol in uppermost Palingkloof Member of Balfour Formation (18.7 m in section of Retallack et al., 2003) at Lootsberg Pass. (c) Sandstone of Kopanskaya Suite above paleosols of Kulchumovskaya Suite at Krasnogor (Mikhail Surkov's head is at 0 m in section of Taylor et al., 2009). (d) Permian calcareous nodular paleosol of Kulchumovskaya Suite at Bovevaya Gora (162 m in section of Taylor et al., 2009). Images c–d are courtesy of Timothy Kearsey.

pedotypes, are needed for two reasons. First, pedotypes provide specific reference profiles for testing alternate hypotheses. For example, Tabor et al. (2007) argued that Permian and Triassic paleosols at Carlton Heights, South Africa, were formerly waterlogged and so unsuitable proxies for atmospheric CO_2 or paleoclimate. The paleosols in question were described (by Retallack et al., 2003) as Sedibo pedotype and their waterlogging acknowledged, but interpretative limitations of those few paleosols do not apply to other pedotypes at Carlton Heights or elsewhere in South African rocks of equivalent age (Fig. 2a–b). Gastaldo et al. (2009) suggested correlation of a laminite unit 8 m above the Permian–Triassic transition laminites at Bethulie, South Africa, but the lower laminites are unmistakably different in grain size (clay–silt versus silt–sand), color (dark red-gray versus light greenish gray) and associated paleosols (Zam versus Barathi pedotypes respectively: Retallack et al., 2003). Pedotype terminology allows precision in paleosol description and naming.

Second, pedotypes represent fundamental interpretive units, each requiring individual interpretation of soil-forming factors. Unlike lake deposits with their confusing mix of leaves from various sources (Gastaldo et al., 2005), paleosols preserve the roots, trunks and leaf litters of plant growing within them (Retallack and Krull, 1999). Poorly drained Triassic paleosols supported lycopsids with hollow roots and corms (*Cylostrobus* on Warriewood pedotype), whereas well drained Triassic paleosols of the same formations supported seed ferns (*Dicroidium* on Avalon pedotype) and conifers (*Voltziopsis* on Long Reef pedotype), with copiously branching woody roots (Retallack, 1997b, 1997c). Similarly bones of vertebrates can be carried by streams far from their habitats (Retallack et al., 2007), but the skeletons of animals buried in their burrows and disarticulated within paleosols are good guides to paleocommunities. For example, South African Kuta pedotype yielded only *Lystrosaurus*, often within burrows (Bordy et al., 2011), but the nearby Patha pedotype included a more diverse assemblage of *Lystrosaurus*, *Proterosuchus*, *Owenetta*, and a whaitsiid carnivore (Retallack et al., 2003). The Permian–Triassic therapsids *Lystrosaurus* and *Diictodon* were burrowers in well drained soils (Kuta and Som pedotypes respectively), and not as was once thought, aquatic

Fig. 3. Calcareous red bed sections of Bernal Mesa, New Mexico (a–b) and Caprock Canyons, Texas (c–d), U.S.A. (a) Red beds of the Bernal Formation overlain by sandstones of the Anton Chico Formation (near top of mesa) viewed from south. (b) Deep-calcic paleosol within upper Bernal Formation (34.6 m in section of Retallack, 2005a). (c) Red beds of Alibates Formation (lowest gully) overlain by Dewey Lake Formation viewed from west. (d) Deep-calcic paleosol within Dewey Lake Formation (11.7 m in section of Retallack, 2005a).

creatures (Smith, 1987; Groenewald, 1991). Likely therocephalian therapsid burrows from the Early Triassic of Antarctica described by Sidor et al. (2008) are common in the Gregory pedotype at 183 m in the section of Retallack and Krull (1999), whereas *Lystrosaurus* and *Thrinaxodon* have been found in Dolores pedotype paleosols elsewhere in Antarctica (Retallack and Hammer, 1998). There are few large collections of Permian and Triassic fossils tied to particular pedotypes, but paleocommunities would be better understood if careful note of associated paleosols were made.

3. Paleoclimatic records

3.1. Paleoprecipitation

Paleoprecipitation can be estimated for paleosols from depth to carbonate nodules (D_o in cm), which increases in modern soils with mean annual precipitation (R in mm) following Eq. (1) below ($R^2 = 0.52$, standard error ± 147 mm). In other words, modern soils with deep calcareous nodular (Bk) horizons form in humid climates and those with shallow nodular horizons in arid climates (Retallack, 2005b).

$$R = 137.24 + 6.45D_o - 0.013{D_o}^2 \quad (1)$$

In using depth to Bk as a proxy for paleoprecipitation, allowance needs to be made for burial compaction of the paleosols, which reduces depth to Bk, using a standard compaction equation (Sheldon and Retallack, 2001). Depths in paleosols can also be compromised by erosion under paleochannels or by vertic displacement, but these effects are avoided by field observations in large outcrops (Retallack et al., 2003). Higher than modern atmospheric CO_2 may increase depth to carbonate nodules in soils, but an increase from 280 to 3080 ppmv modeled by McFadden and Tinsley (1985) increased depth to pedogenic carbonate only 5 cm, so this correction is seldom necessary. Another control of depth to Bk in modern soils is respired CO_2 in the soil, a measure of secondary productivity, but this is closely correlated with mean annual precipitation in modern soils (Retallack, 2009b). Permian and Triassic ecosystems do not appear to have been

so physiognomically distinct from modern vegetation to require a productivity correction, but such corrections may be needed for Devonian and geologically older paleosols (Retallack and Huang, 2011).

Another useful paleohyetometer for paleosols was devised by Sheldon et al. (2002) based on chemical index of alteration without potash ($CIA-K=A=100\ mAl_2O_3/(mAl_2O_3+mCaO+mNa_2O)$, in moles), which increases with mean annual precipitation (R in mm) in modern soils ($R^2=0.72$; S.E. $=\pm 182$ mm), as follows.

$$R = 221e^{0.0197A} \quad (8)$$

This formulation is based on the hydrolysis equation of weathering, which enriches alumina at the expense of lime, magnesia, potash and soda. Magnesia is ignored because it is not significant for most sedimentary rocks, and potash is left out because it can be enriched during deep burial alteration of sediments (Maynard, 1992). One limitation of this method is that it conflates weathering that contributed to production of sedimentary parent material with weathering within the paleosol: full profile mass balance may be needed to address this problem (Retallack and Huang, 2011). Another problem in application to calcareous paleosols is that the proxy was devised only for non-calcareous parts of paleosols, not calcareous nodules which can be tiny and scattered in their distribution: any analysis with more than 3 wt.% CaO should be not be used as a proxy.

Such estimates of paleoprecipitation for Permian and Triassic calcareous paleosols are presented in Fig. 4b–d using the Bk proxy, and for non-calcareous paleosols in Fig. 4e using the CIA − K proxy. The Sydney Basin sequence includes coal measures of a more humid region (Retallack et al., 2011) than the aridlands represented by Utah (Retallack, 2009a), Texas (Retallack, 2005a) and South Africa (Retallack et al., 2003). The Karoo Basin was the driest of these regions, and has indications of loess and declining precipitation to the east as in the Karoo desert today (Retallack et al., 2003). Despite regional differences and some intervals of sparse or missing data (uninflected parts of time series in Fig. 4), the principal spikes in paleoprecipitation appear synchronous globally.

Other aspects of paleoprecipitation, such as seasonality can be inferred from spread of carbonate nodules within profiles: modern monsoonal soils have carbonate nodules widely spread though the profile, whereas soils with less seasonal precipitation have more focused horizons of nodules (Retallack, 2005b). Results of such observations for Permian and Triassic paleosols of Utah and New Mexico did not show increased monsoonal seasonality at times of high CO_2 (Retallack, 2009a). Monsoonal seasonality requires particular local geographic contrasts between land and sea temperatures (Solomon et al., 2007).

Another approach to paleoseasonality is the use of soil morphology as well as geochemical proxies for evapotranspiration and energy input from precipitation to estimate vegetation types. Application of these proxies for earliest Permian paleosols of Texas and New Mexico found basal and mid Asselian, and lower Sakmarian spikes in paleoprecipitation represented by wet forests, in contrast to other times of moist forest and desert shrubland (Gulbranson et al., 2011).

3.2. Paleotemperature

A useful paleotemperature proxy for paleosols devised by Sheldon et al. (2002) uses alkali index ($N=(K_2O+Na_2O)/Al_2O_3$ as a molar ratio), which is related to mean annual temperature (T in °C) in modern soils by Eq. (2) ($R^2=0.37$; S.E. $=\pm 4.4$ °C). This inverse relationship may reflect increase alkali mobilization in warm soils.

$$T = -18.52\,N + 17.22 \quad (2)$$

Such estimates of paleotemperature for Permian and Triassic paleosols are presented in Fig. 5b–c. These data show spikes in paleotemperature corresponding to most of the spikes in paleoprecipitation (Bk proxy Fig. 5a). Paleotemperatures for Sydney Basin (Fig. 5c) non-calcareous paleosols are reasonable for such a high-latitude site, but those for paleotropical Utah–New Mexico (Fig. 5b) are unrealistically low, and may indicate that this proxy was compromised by salt precipitation in semiarid climates, which were poorly represented in the training set of modern soils (Sheldon et al., 2002). Study of phyllosilicate and hematite isotopic composition (δD and $\delta^{18}O$) in Late

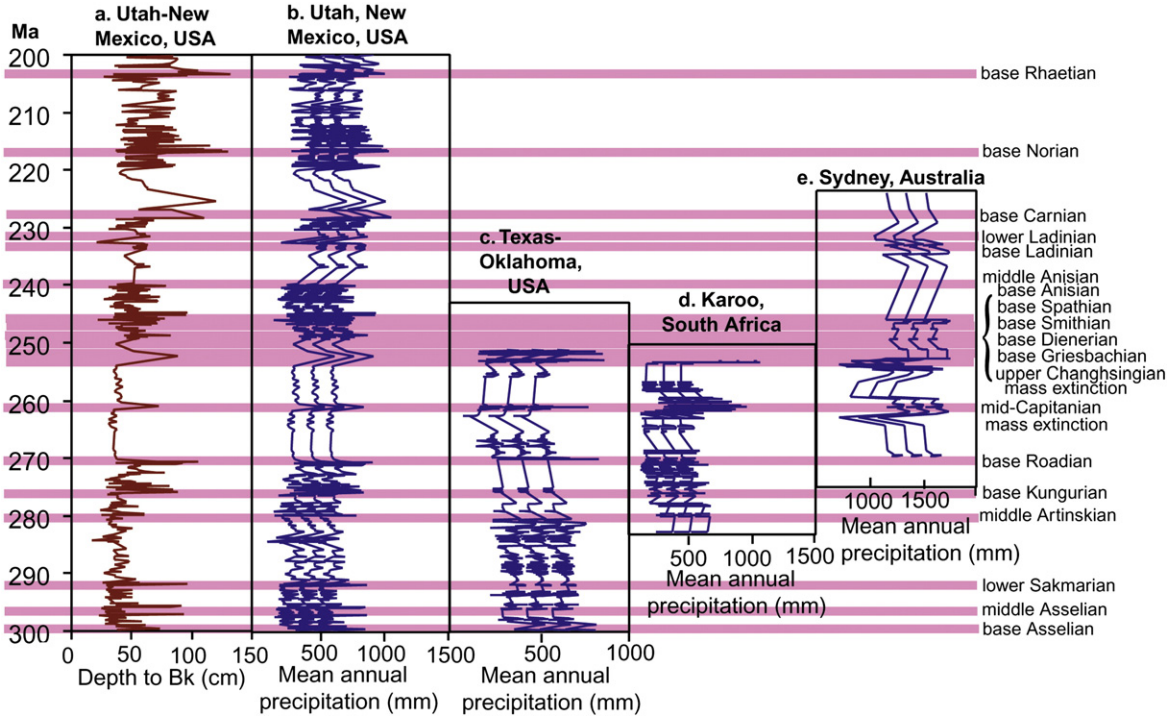

Fig. 4. Utah–New Mexico paleoclimatic proxy record (after Retallack, 2009a) compared with paleoprecipitation estimated for compaction-corrected depth to Bk in Utah–New Mexico (Retallack, 2009a), Texas–Oklahoma and South Africa (Retallack, 2005a), and from analysis for chemical index of alteration minus potash in the Sydney, Australia (Retallack et al., 2011).

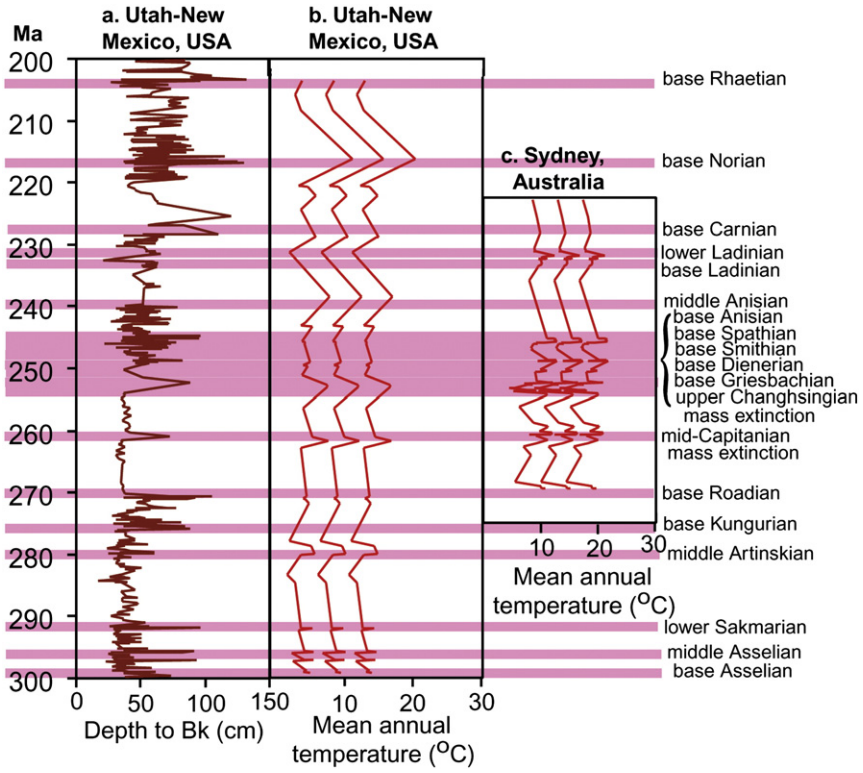

Fig. 5. Utah–New Mexico paleoclimatic proxy record (after Retallack, 2009a) compared with paleotemperature time series estimated from chemical analysis for alkali index in Utah–New Mexico (Retallack, 2009a), and Sydney Australia (Retallack et al., 2011).

Pennsylvanian–Early Permian (305–280 Ma) paleosols of nearby Texas have been taken as evidence of paleotemperatures of 24–37 °C, with abrupt rises in the basal and middle Asselian (Tabor, 2007). Comparable earliest Triassic temperature rises have been proposed from oxygen isotopic depletion in tropical marine carbonates from China (Joachimski et al., 2012). These isotopic analyses are evidence that some paleoclimatic spikes were oppressively hot in the tropics.

4. CO_2 greenhouse proxies

The CO_2 paleobarometer of Retallack (2009a) can be used to estimate atmospheric CO_2 (C in ppmv) from stomatal index (I in %) of fossil plants with preserved cuticles. Eq. (3) for atmospheric CO_2 was based on greenhouse experimental data with living *Ginkgo* and on counting of herbarium specimens of *Ginkgo* collected during the rapid and ongoing post-industrial rise of atmospheric CO_2. *Ginkgo* is found in Late Triassic and later rocks, but fossil seed ferns such as *Lepidopteris* have comparable stomatal structure to living *Ginkgo* and similar stomatal index to *Ginkgo* when found within the same deposits (Retallack, 2002). This inverse relationship quantifies the observation that plant leaves have fewer stomates when atmospheric CO_2 is high than when atmospheric CO_2 is low, because stomates also mitigate water loss (Wynn, 2003).

$$C = 294.1 + \left[\frac{1}{(4.84 \times 10^{-10})I^{7.93}}\right] \quad (3)$$

The compilation of Permian and Triassic CO_2 determinations from stomatal index of fossil *Lepidopteris* shown in Fig. 6b and Table 3 is mainly from Retallack (2009a), with additions from Vörding and Kerp (2008), Chaney et al. (2009), Bonis et al. (2010), Bomfleur et al. (2011b), and Retallack et al. (2011). The highest calculated levels of CO_2, a staggering 7832 ± 1676 ppm (2σ error by Gaussian propagation) at the Late Permian mass extinction horizon is 28 times the postglacial–preindustrial CO_2 levels of 280 ppmv (Solomon et al., 2007). Most of the paleoclimatic transients identified in Utah–New Mexico (Fig. 6a) are represented by spikes in atmospheric CO_2 (Fig. 6b). Also found are numerous intervening times when CO_2 was a near modern 300–500 ppmv (Fig. 6b). Modern CO_2 values are rising: the year 2011 peaked at 394 ppm in June at Mauna Loa, Hawaii (Tans and Keeling, 2011).

Organic carbon isotopic data for the Permian and Triassic can also be regarded as an indirect proxy for atmospheric CO_2 because extremely low isotopic values can only be plausibly explained using isotopic mass balance by atmospheric injection of large amounts of isotopically light CH_4 (Krull and Retallack, 2000; Retallack and Jahren, 2008). Unusually large negative isotopic excursions have been found at 122 Permian–Triassic boundary sections around the world (Korte and Kozur, 2010). Methane itself is a potent greenhouse gas, and in addition would have oxidized to CO_2 within a decade (Solomon et al., 2007). These isotopic records are thus indirect evidence for volatility of atmospheric greenhouse gas composition, and the unusual magnitude of Permian–Triassic boundary events. Because abundant methane is indicated by very negative isotopic values (Krull and Retallack, 2000), spikes in CO_2 levels from stomatal index (Fig. 6b) and in the Bk paleoclimatic proxy (Fig. 6a) correspond with troughs in isotopic composition of organic matter (Fig. 6c). This is only an indicator of greenhouse extremes, because other factors come into play at moderate carbon isotopic compositions (Retallack and Jahren, 2008; Korte and Kozur, 2010). For example, another unusual characteristic of the isotopic composition of Permian fossil plants is an increased difference in carbon isotopic composition compared with coeval marine carbonate ($\Delta^{13}C$), and this has been used by Beerling et al. (2002) to confirm model results of Berner (2006) suggesting atmospheric O_2 high as 35% during the Late Carboniferous and Permian, but much less (16%) during the early Triassic.

Atmospheric CO_2 can also be estimated from carbon isotopic composition of paleosol carbonate and organic matter, because there is a marked difference in isotopic compositions of carbon in CO_2 of open

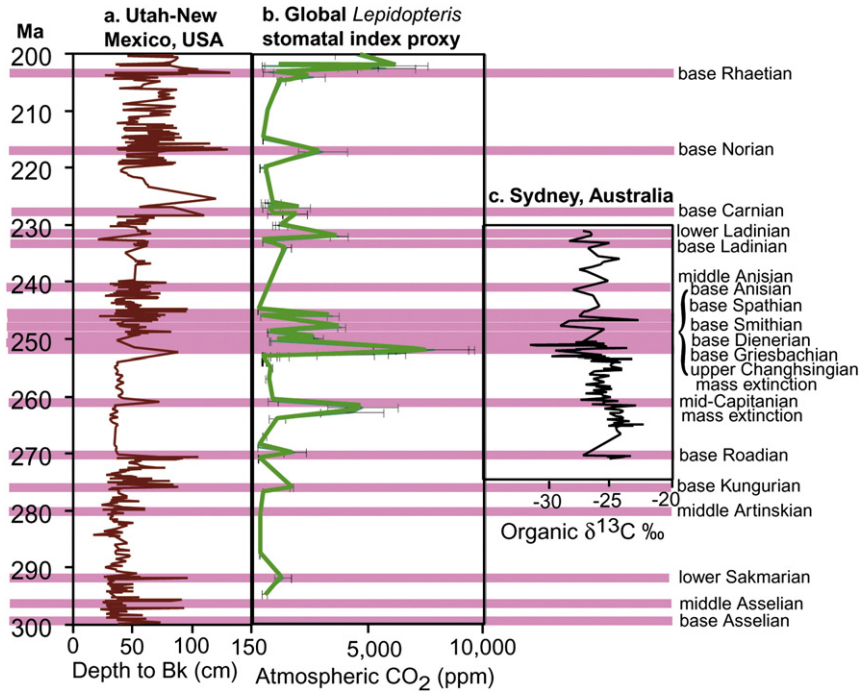

Fig. 6. Utah–New Mexico paleoclimatic proxy record (after Retallack, 2009a) compared with carbon dioxide estimates across the Permian–Triassic boundary from *Lepidopteris* stomatal index (Retallack, 2009a; Bonis et al., 2010; Retallack et al., 2011) and carbon isotope composition of organic matter in the Sydney Basin, Australia (after Retallack et al., 2011).

air (about −6.5‰ $\delta^{13}C$) and respired in soil air (about −26‰ $\delta^{13}C$ in model soil of Cerling, 1991). At times of high atmospheric CO_2, diffusion of isotopically heavy atmospheric CO_2 into a soil with isotopically light respired CO_2 increases the isotopic value fixed within low magnesium calcite of soil carbonate. These calculations require not only (1) carbon isotopic composition of carbonate, but (2) atmospheric CO_2 isotopic composition from paleosol organic matter (Arens et al., 2000), which may have to be modeled to offset effects of plant decomposition (Wynn, 2007), (3) paleotemperature from paleosol chemical composition (Sheldon et al., 2002) or oxygen isotope ($\delta^{18}O$) composition of phyllosilicates (Tabor, 2007) or carbonate (Dworkin et al., 2005), and (4) respired soil CO_2 concentrations from depth to paleosol Bk (Retallack, 2009a) corrected for burial compaction (Sheldon and Retallack, 2001). These complex equations are difficult for the Permian Triassic boundary interval when atmospheric carbon isotopic composition fluctuated so wildly, but nevertheless the few pedogenic estimates available confirm both spikes of about 5000 ppm for the Permian–Triassic transition (Thomas et al., 2007) and 1300–1600 ppm for early Late Triassic (Prochnow et al., 2006), as well as other times when CO_2 was an unremarkable 300–500 ppm (Ekart et al., 1999; Montañez et al., 2007).

Another indication of elevated atmospheric CO_2 may be pedogenic dolomite nodules, because most modern soils and paleosols from times of low atmospheric CO_2 have low magnesian calcite nodules (Retallack, 2009a; Kearsey et al., 2012). The reason for this temporal correlation has been unclear until recently. Now, Zhang et al. (2012) report the formation of disordered dolomite at room temperature by the dehydrating action of sugars derived from extracellular

Table 3
Permian–Triassic greenhouse crises, events and non-marine Lagerstätten.

Ma	Geological age	$_pCO_2$ (ppmv)	Notable and other events	Non-marine Lagerstätten	References
203.6	Base Rhaetian	6121	Lepidosuars and testudines diversify	Redonda	Johnson et al., 2002
216.5	Base Norian	3074	Mammals and dinosaurs diversify	Solite	Olsen and Johansson, 1994
228.0	Base Carnian	1887	Phytosaurs and cheirolepid conifers diversify	Madygen	Grimaldi and Engel, 2005
236.0	Lower Ladinian	1517	Gnetaleans diversify	St. Peters	Woodward, 1908
237.0	Base Ladinian	(≈1600)	End of coal gap	Brookvale	Wade, 1935
242.0	Middle Anisian	(≈2000)	Bennettites diversify	Sidmouth	Benton and Spencer, 1995
246.8	Base Anisian	3860	Rhynchosaurs and pteridosperms diversify	Hangviller	Etter, 2002
250.8	Base Spathian	(≈3000)	Pleuromeialian acme	Gosford	Woodward, 1890
251.5	Base Smithian	(≈3000)	Pleuromeialian acme	Velikhorestskoe	Shishkin et al., 2000
252.0	Base Dienerian	2882	Pleuromeialian acme	Vikundu	Hankel, 1992
252.1	Lower Griesbachian	7243	Pleuromeialian acme	Maji ya Chumvi	Hankel, 1992
252.3	Upper Changhsingian	7832	Mass extinction, Siberian Traps, coal gap	Anakit	Shishkin, 1998
262.0	Middle Capitanian	4766	Mass extinction, Emeishan Traps, end P4	Rapid City	Hussakof, 1916
270.6	Lower Roadian	1887	End of pelycosaurs, coal flora, P3 glaciation	Koštálov	Milner, 1981
275.6	Lower Kungurian	1745	Voltzialean conifers diversify	Tschekarda	Grimaldi and Engel, 2005
280.0	Middle Artinskian	(≈1000)	End P2 glaciaton: lakes with *Mesosaurus*	Worcester	MacRae, 1999
292.0	Lower Sakmarian	1369	End P1 glaciation	Elmo	Grimaldi and Engel, 2005
297.0	Middle Asselian	(≈1500)	Lakes with *Micromelerpeton*	Odernheim	Witzmann and Pfritzschner, 2003
299.0	Lower Asselian	(≈1000)	Lakes with jellyfish	Gottlob	Gand et al., 1996

Note: The pCO_2 estimates are from stomatal index of *Lepidopteris* (Retallack, 2009a; Bonis et al., 2010; Retallack et al., 2011), but those in round numbers are interpolated from relative strength of paleoclimatic proxy (Retallack, 2009a). Glaciations (P1–4) are after Fielding et al. (2008). Plant events are from Anderson et al. (2007) and vertebrate events from Benton (1983).

polysaccharides of microbes. This effect is more marked with galactose from methanogens, sulfur reducing and fermenting bacteria than with glucose from cyanobacteria and plants, implying that greenhouse spike aridland soils have different microbial communities than icehouse aridland soils.

Other proxies for former atmospheric CO_2 include mass balance models of sedimentary carbon and sulfur (Berner, 2006), and strontium isotopic values of marine carbonates (Rothman, 2002), but these marine records calculated in steps of 10 million years misleadingly show long periods of very high CO_2, unlike the transient spikes apparent from pedogenic carbonate (Prochnow et al., 2006) and stomatal index data (Fig. 6). Marine algal carbon isotope composition (Kaufman and Xiao, 2003; Freeman and Pagani, 2005), and base depletion of paleosols (Sheldon, 2006), have low precision, but have been usefully applied to unusually high levels of Precambrian CO_2. Alkenone organic carbon compared with foraminiferal carbonate carbon isotopes (Freeman and Pagani, 2005), and foraminiferal boron isotopes (Pearson and Palmer, 1999) have been applied to Cenozoic records only, because they are vulnerable to organic thermal maturation and carbonate diagenesis. The alkenone and boron proxies are compromised by variations in river input to the ocean (Royer et al., 2001). Goethite-occluded carbonate in paleosols can also be used as CO_2 proxy (Tabor and Yapp, 2005), but it is rarely preserved in paleosols as old as Permian and Triassic because of burial dehydration of goethite to hematite (Retallack, 1997a, 2001).

5. Vegetation crises

The Late Permian (upper Changhsingian) mass extinction terminated glossopterids, gigantopterids, tree lycopsids and cordaites, which were major contributors to coals in the southern hemisphere, China, and northern hemisphere, respectively (Sadovnikov and Orlova, 1990; Wang, 1996; Retallack et al., 2006; Shen et al., 2011). This mass extinction of wetland plants was at a time of unusually anoxic swamp soils (Sheldon and Retallack, 2002), and ushered in a 15 million year hiatus in peat formation ("coal gap" of Retallack et al., 1996). Other Permian and Triassic greenhouse events also correspond to stages in evolution of wetland floras: Early Permian *Callipteris–Ottokaria* flora, Middle Permian *Plumsteadia–Rufloria* flora, Late Permian *Lidgettonia–Tatarina* flora, latest Permian–Early Triassic *Pleuromeia* flora, and Middle–Late Triassic *Dicroidium–Scytophyllum* flora (*Ottokaria*, *Plumsteadia* and *Lidgettonia* are reproductive structures attached to *Glossopteris* leaves; Dobruskina, 1980; Meyen, 1982; Retallack, 2005a; Retallack et al., 2006). Early Permian vegetation was decidedly archaic, with broadleaf seed ferns and tree lycopsids not much different from Carboniferous swamp vegetation, but by the Late Triassic, modern clades of conifers, cycads and gnetaleans were diverse (Anderson et al., 2007; DiMichele et al., 2008; Xiong and Wang, 2011).

Greenhouse events were not only turning points in plant evolution, but also promoted transient crisis vegetation. A narrow horizon of conifer-dominated floras from the basal Middle Permian (Roadian) of Texas for example is anomalous within a sequence dominated by broadleaved seed ferns (DiMichele et al., 2001). Greenhouse warming in this paleotropical region may have created evapotranspiration levels intolerable to many broadleaved plants. Other greenhouse transients of latest Permian to Early Triassic floras worldwide are represented by assemblages of non-arborescent isoetalean lycopsids, including the oldest known fossils of the living genus *Isoetes* (Retallack, 1997c; Naugolnykh and Mogutcheva, 2006), and a variety of allied extinct genera such as *Pleuromeia*, *Cylostrobus*, *Tomiostrobus*, *Gagariostrobus* and *Mesenteriophyllum* (Wang, 1996; Mogutcheva and Naugolnykh, 2010; Bomfleur et al., 2011a; Sadovnikov, 2011). The large apical meristem of these plants would have made them frost sensitive, like modern palms and cacti (Retallack et al., 2011), and yet they are locally common with high paleolatitude floras of southeastern Australia (Retallack, 1997c) and Siberia (Sadovnikov, 2011). Greenhouse warming events may have enabled dispersal from tropical to polar regions.

In the high paleolatitude Sydney Basin, Australia, times of greenhouse crisis (Fig. 7a) coincided with spikes of lycopsid spore diversity (Fig. 7b) and large diameter leafy axes (Fig. 7c). Most (but not all) of

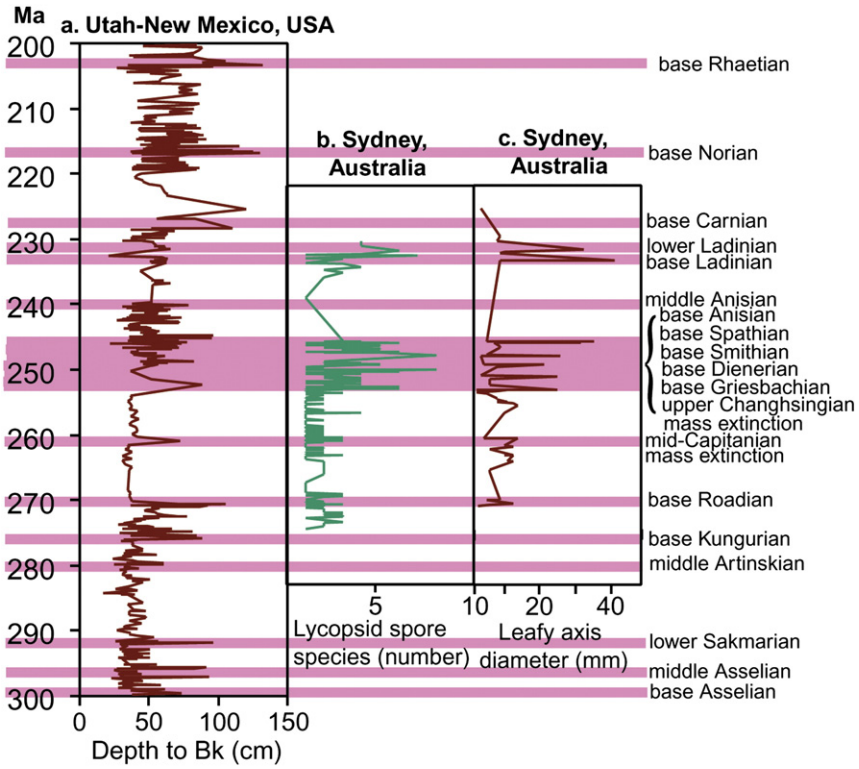

Fig. 7. Utah–New Mexico paleoclimatic proxy record (after Retallack, 2009a) compared with spikes in diversity of tropical lycopsid spores and of plants with large leafy axes, and thus frost sensitive terminal meristems in the Sydney Basin, Australia (after Retallack et al., 2011).

these large leafy axes and lycopsid spores were isoetaleans (Retallack et al., 2011), which are restricted to particular narrow horizons (Retallack, 1997c). There are comparable successive acme zones of *Tomiostrobus* in Siberia (Sadovnikov, 2011) and of *Pleuromeia* in North China (Wang, 1996). Intervening strata between these lycopsid spikes are dominated by conifers, seed ferns, ferns and horsetails, which represent the normal high-latitude floras of those regions. Thus Permian and Triassic greenhouse spikes were responsible for widespread but transient distribution of thermophilic lycopsids, on unusually short time scales during the Early Triassic. The long recovery from Late Permian (late Changsingian) mass extinction was not simply due to its unusual severity, but due to repeated Early Triassic greenhouse crises (Retallack et al., 2011).

6. Animal crises

The Late Permian (upper Changhsingian) mass extinction terminated gorgonopsian therapsids (Ward et al., 2005), the Middle Permian (mid-Capitanian) mass extinctions terminated dinocephalian therapsids (Retallack et al., 2006), and both events strongly reduced vertebrate biodiversity (Rubidge, 1995; Fröbisch, 2008). These events together with basal Wordian and basal Carnian greenhouse events punctuate dynasties of Permian–Triassic vertebrates: Early Permian pelycosaur, Middle Permian dinocephalian, Permian–Triassic dicynodont, Middle Triassic rhynchosaur and Late Triassic dinosaur faunas. Early Permian pelycosaur faunas included archaic reptiles and amphibians not much different from those of Carboniferous coal swamps, but by the Late Triassic there were already a variety of small mammals and large dinosaurs (Benton, 1983, 2008; Kitching and Raath, 1984; Benton et al., 2004; Lucas, 2006, 2009).

Greenhouse crises may also have played a role in mass extinctions and long-term evolutionary trends. Not only would greenhouse gases have disrupted life on land with warmer and wetter climates, but with spreading tropical pathogens, long-distance plant and animal migrations, sea level rise, groundwater hypoxia and water acidification (Retallack, 2011). In addition, atmospheric oxygen depleted by massive emissions of CH_4 and H_2S (Berner, 2006) would have challenged animals with pulmonary edema and other maladies of mountain sickness familiar to mountaineers today (Retallack et al., 2003; Engoren and Retallack, 2004). High elevations may have become uninhabitable, further reducing habitat for many animals (Huey and Ward, 2005). *Lystrosaurus*, notable as one of the few survivors of the Late Permian mass extinction (Botha and Smith, 2007), shows a variety of adaptations to low oxygen atmosphere (Retallack et al., 2003): small–medium body size, secondary bony palate, barrel chest, short rib cage (supporting a muscular diaphragm?), and short muscular limbs (allowing burrowing: Groenewald, 1991).

Fig. 8 shows that both upper Changhsingian and mid-Capitanian mass extinctions were turning points in long-term evolution of respiratory adaptations in South African Permian–Triassic and South American Late Triassic anomodont therapsids (data from Angielczyk and Walsh, 2008). Both greenhouse and mass extinctions events curtailed a long-term increase in body size (Fig. 8d), and were followed by marked advances in area of both the secondary bony palate (Fig. 8c) and internal nares (Fig. 8d). The bony secondary palate separates the buccal from the nasal cavity, thus creating an airway unobstructed by tongue or food. Increased area of the bony secondary palate expanded to cover areas that were internal nares in Early Permian therapsids, but the area of internal nares remained little changed because of increases in body size through time (Fig. 8).

A long term shift from the sprawling gait of crocodilians to the more erect gait of mammals is seen within Permian and Triassic fossil trackways (Kubo and Benton, 2009). Within dicynodonts this transition was completed by the latest Permian Coal Cliff Sandstone (Retallack, 1996; Retallack et al., 2011).

7. Conclusions

Numerous CO_2 greenhouse spikes are now recognized during the Permian and Triassic (Table 3), and these have consequences for stratigraphy and paleontology, as shown in Fig. 9 for sections in Australia,

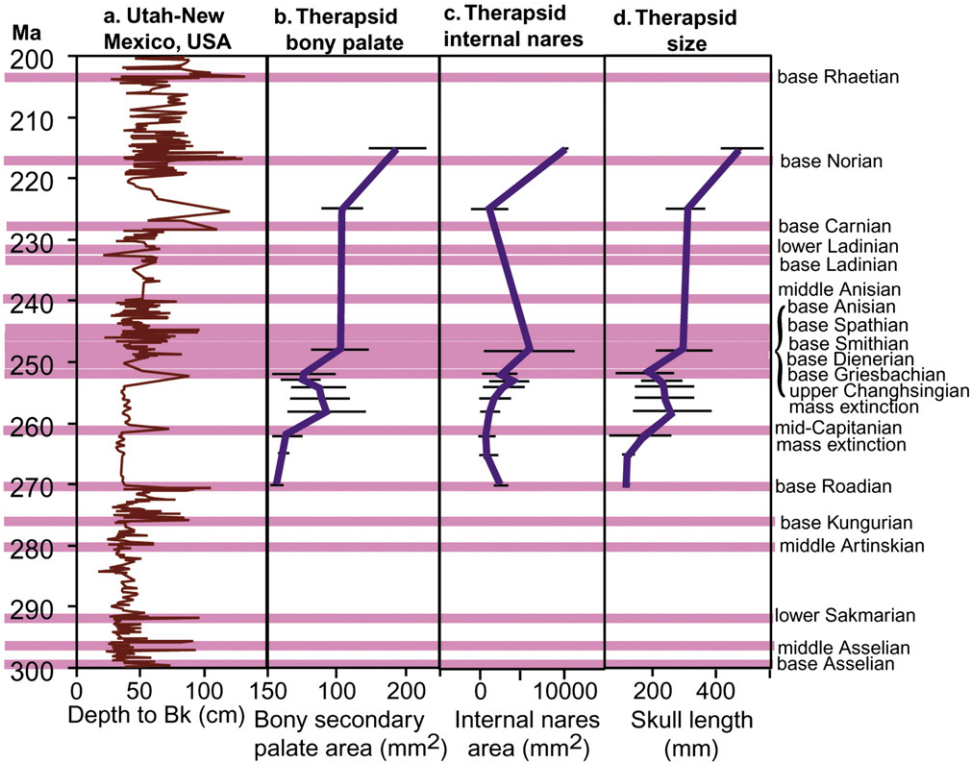

Fig. 8. Utah–New Mexico paleoclimatic proxy record (after Retallack, 2009a) compared with Permian–Triassic changes in respiratory adaptations of anomodont therapsid synapsids (data from Angielczyk and Walsh, 2008).

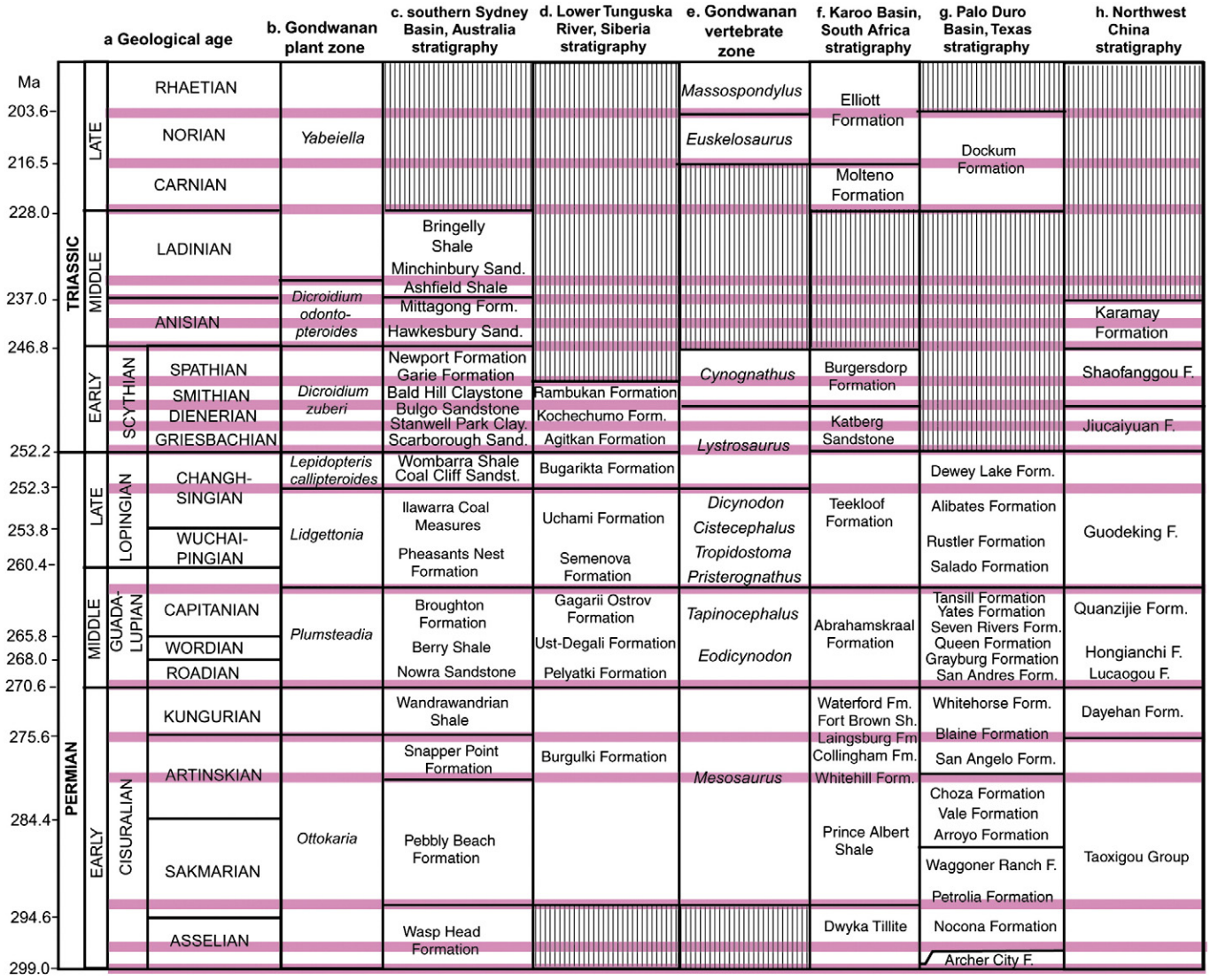

Fig. 9. International correlations of Permian and Triassic greenhouse crises.
Data sources for columns are. a) Gradstein et al. (2004), Ovtcharova et al. (2006). Shen et al. (2011) b) Retallack (2005a). c) Retallack et al. (2011). d) Meyen (1982), Sadovnikov (2008), Sadovnikov and Orlova (1990), Kozur and Weems (2011). e–f) Kitching and Raath (1984), Rubidge (1995). g) Retallack (2005a). h) Thomas et al. (2011).

in Australia, Siberia, South Africa, Texas and northwest China. Greenhouse spikes were times of marine transgression (Retallack, 2011) and of braided rather than meandering streams (Retallack, 1999; Ward et al., 2000), with widespread stratigraphic consequences. Greenhouse crises also terminated glacial episodes (Fielding et al., 2008). Greenhouse spikes were also times of lycopsid acme zones (Retallack, 1997c). Many famous Permian and Triassic fossil deposits for articulated fish and insects coincide with greenhouse crises (Woodward, 1890, 1908; Hussakof, 1916; Wade, 1935; Milner, 1981; Hankel, 1992; Olsen and Johansson, 1994; Benton and Spencer, 1995; Gand et al., 1996; Shishkin, 1998; MacRae, 1999; Shishkin et al., 2000; Etter, 2002; Johnson et al., 2002; Witzmann and Pfritzschner, 2003; Grimaldi and Engel, 2005). Greenhouse crises enhance a variety of preservative conditions, such as high sea level, greater magnitude of storms and floods, and acidification and anoxia of groundwater (Retallack, 2011). Greenhouse crises were survived by small to medium vertebrates capable of burrowing and coping with low oxygen (Retallack et al., 2003). In sequences of red calcareous paleosols (Figs. 2–3), greenhouse crises are marked by deep-calcic well-developed clayey paleosols (Retallack, 2009a). In sequences of coal measures, greenhouse crises are marked by paleosols with siderite and berthierine indicative of hypoxia (Retallack, 1997b; Sheldon and Retallack, 2002). By altering both climate and groundwater, CO_2 greenhouse spikes had varied biotic and sedimentary consequences that have yet to be considered in many sequences.

Terminological problems arise from the fact that Middle to Late Permian mass extinctions and greenhouse horizons are not at the end of Middle or Late Permian (Kozur and Weems, 2011). It has become customary to talk of “end-Permian” (Shen et al., 2011) and “end-Guadalupian” extinctions (Clapham et al., 2009). The stratigraphic gap between the lowest basal Triassic conodont *Hindeodus parvus* and extinction and carbon isotopic evidence of greenhouse crisis in the stratotype section at Meishan, China, is only 17 cm, which is now thought to represent 200,000 years (Shen et al., 2011). However this interval can be estimated from carbon isotope chemostratigraphy as 10 m near Hovea, western Australia (Metcalfe et al., 2008; Shi et al., 2010), 18 m in South Africa (Retallack et al., 2003), 20 m at Caprock Canyons, Texas (Retallack, 2005a), 40 m near Muswellbrook, in southeastern Australia (Retallack et al., 2011), 40 m in northwest China (Metcalfe et al., 2009; Thomas et al., 2011) and 50 m at Graphite Peak, Antarctica (Krull and Retallack, 2000). Middle Permian mass extinction

in stratotype sections of China is now considered mid-Capitanian rather than end-Capitanian (= end-Guadalupian: Wignall et al., 2009). The end-Guadalupian in China is now dated at 259 Ma (Shen et al., 2010) and the Emeishan flood basalts at 257 ± 9 Ma (Lai et al., 2012). An age of 262 rather than 259 Ma is likely for the mid-Capitanian glossopterid mass extinction in Antarctica (Retallack et al., 2006) and southeastern Australia (Retallack et al., 2011), and dinocephalian extinction in South Africa (Retallack et al., 2006) and Russia (Lucas, 2009). These differences arise because Middle and Late Permian and Triassic are defined by first appearances of conodonts, not mass extinctions (Henderson, 2005).

Permian and Triassic greenhouse spikes are of special interest because they include two of the greatest greenhouse crises of the Phanerozoic (upper Changhsingian and mid Capitanian), and a variety of less severe greenhouses (Figs. 4–8). Such an array of cases can be used to examine a variety of hypotheses about climatic and biotic consequences of spikes in atmospheric CO_2. Will such CO_2 increases result in wetter local climates? Will CO_2 rises result in warmer climate? Will CO_2 rises promote poleward dispersal of thermophilic plants? Will CO_2 rises select for improved vertebrate respiration? Data presented here (Figs. 4–5 and 7–8) answers all these questions in the affirmative, but more could be done to quantify the effects of CO_2 from such data. Comparable data has been used for the Utah–New Mexico time series (Retallack, 2009a), to determine empirically that CO_2-temperature sensitivity (MAT change with CO_2 doubling) for that region is 0.8 °C. This was the first such estimate based on empirical paleoproxy data, and the estimate is low compared with global sensitivity determined by modeling studies (1.5–6.2 °C: Royer et al., 2007). Similar data from the Utah–Mexico time series was used to determine CO_2-precipitation sensitivity (MAP increase for CO_2 doubling) of 89 mm for calcic horizon estimates and 128 mm for geochemical estimates (Retallack, 2009a). These studies are preliminary indications of what can be learned from such data on past consequences of elevated atmospheric CO_2.

Acknowledgments

Peter Ward facilitated fieldwork in South Africa. Lisa Emerson aided fieldwork in Utah and Wyoming. Douglas Ekart, Neil Tabor, John Geissman, Bob Gastaldo and Nathan Sheldon offered helpful discussions. Fieldwork in Antarctica was funded by NSF grants OPP9315228 and 0230086.

References

Anderson, J.M., Anderson, H.M., Cleal, C.J., 2007. Brief history of the gymnosperms: classification, biodiversity, phytogeography and ecology. Strelitzia 20 279 pp.

Angielczyk, K.D., Walsh, M.L., 2008. Patterns in the evolution of nares size and secondary palate length in anomodont therapsids (Synapsida): implications for hypoxia as a cause for end-Permian terrestrial vertebrate extinctions. Journal of Paleontology 82, 528–542.

Arens, N.C., Jahren, A.H., Amundson, R., 2000. Can C3 plants faithfully record the carbon isotopic composition of atmospheric carbon dioxide? Paleobiology 26, 137–164.

Becker, L., Poreda, R.J., Hunt, A.G., Bunch, T.E., Rampino, M., 2001. Impact event at the Permian–Triassic boundary: evidence from extraterrestrial noble gases in fullerenes. Science 291, 1530–1533.

Becker, L., Poreda, R.J., Basu, A.R., Pope, K.O., Harrison, T.M., Nicholson, C., Iaksy, R., 2004. Bedout: a possible end-Permian impact crater offshore of northwestern Australia. Science 304, 1469–1476.

Beerling, D.J., Lake, J.A., Berner, R.A., Hickey, L.J., Taylor, D.W., Royer, D.L., 2002. Carbon isotope evidence implying high O_2/CO_2 ratios in the Permo–Carboniferous atmosphere. Geochimica et Cosmochimica Acta 56, 3757–3767.

Benton, M.J., 1983. Dinosaur success in the Triassic: a noncompetitive ecological model. The Quarterly Review of Biology 58, 29–55.

Benton, M.J., 2008. Presidential address 2007: the end-Permian mass extinction — events on land in Russia. Geologists Association Proceedings 119, 119–136.

Benton, M.J., Spencer, P.S., 1995. Fossil Reptiles of Great Britain. Chapman and Hall, London. 386 pp.

Benton, M.J., Tverdokhlebov, V.P., Surkov, M.V., 2004. Ecosystem remodelling among vertebrates at the Permian–Triassic boundary in Russia. Nature 432, 97–100.

Benton, M.J., Newell, A.J., Khlyupin, A.Y., Shurnov, I.S., Price, G.D., Kurkin, A.A., 2012. Preservation of exceptional vertebrate assemblages in Middle Permian fluviolacustrine mudstones of Kotel'nich, Russia: stratigraphy, sedimentology and taphonomy. Palaeogeography Palaeoclimatology Palaeoecology 319–320, 58–83.

Berner, R.A., 2006. GEOCARBSULF; a combined model for Phanerozoic atmospheric O_2 and CO_2. Geochimica et Cosmochimica Acta 70, 5653–5664.

Bomfleur, B., Krings, M., Taylor, E.L., Taylor, T.N., 2011a. Macrofossil evidence for pleuromeialean lycophytes from the Triassic of Antarctica. Acta Palaeontologica Polonica 56, 195–203.

Bomfleur, B., Taylor, E.L., Taylor, T.N., Serbet, R., Krings, M., Kerp, H., 2011b. Systematics and paleoecology of a new Peltaspermalean seed fern from the Triassic polar vegetation of Gondwana. International Journal of Plant Sciences 172, 807–835.

Bonis, N.R., Van Konijnenburg-Van Cittert, J.H.A., Kürschner, W.M., 2010. Changing CO_2 conditions during the end-Triassic inferred from stomatal frequency analysis on *Lepidopteris ottonis* (Goeppert) Schimper and *Ginkgoites taeniatus* (Braun) Harris. Palaeogeography Palaeoclimatology Palaeoecology 295, 146–161.

Bordy, E.M., Sztano, O., Rubidge, B.S., Bumby, A., 2011. Early Triassic vertebrate burrows from the Katberg Formation of the south-western Karoo Basin, South Africa. Lethaia 44, 33–45.

Botha, J., Smith, R.M.H., 2007. *Lystrosaurus* species composition across the Permo–Triassic boundary in the Karoo Basin of South Africa. Lethaia 40, 125–137.

Cerling, T.E., 1991. Carbon dioxide in the atmosphere: evidence from Cenozoic and Mesozoic paleosols. American Journal of Science 291, 377–400.

Chaney, D.S., Mamay, S.H., DiMichele, W.A., Kerp, H., 2009. *Auritifolia* gen. nov., probable seed plant foliage with comioid affinities from the Early Permian of Texas, U.S.A. International Journal of Plant Science 270, 247–266.

Clapham, M.E., Shen, S.-Z., Bottjer, D.J., 2009. The double mass extinction revisited: reassessing the severity, selectivity and causes of the end-Guadalupian biotic crisis (Late Permian). Paleobiology 31, 32–50.

Coney, L., Reimold, W.U., Hancox, P.J., Mader, D., Koeberl, C., McDonald, I., Struck, U., Vajda, V., Kamo, S.L., 2007. Geochemical and mineralogical investigation of the Permian–Triassic boundary in the continental realm of the southern Karoo Basin, South Africa. Palaeoworld 16, 67–104.

Dal Corso, J., Mietto, P., Newton, R.J., Pancost, R.D., Preto, N., Roghi, G., Wignall, P.B., 2012. Discovery of a major negative $\delta^{13}C$ spike in the Carnian (Late Triassic) linked to the eruption of Wrangellia flood basalts. Geology 40, 79–83.

Davies, C., Allen, M.B., Buslov, M.M., Safonova, I., 2010. Deposition in the Kuznetsk Basin, Siberia: insights into the Permian–Triassic transition and the Mesozoic evolution of Central Asia. Palaeogeography Palaeoclimatology Palaeoecology 295, 307–322.

de Wit, M.J., Ghosh, J.G., de Villiers, S., Kakotosolofo, N., James, A., Tripathi, A., Looy, C., 2002. Multiple organic carbon isotope reversals across the Permo–Triassic boundary of terrestrial Gondwana sequences; clues to extinction patterns and delayed ecosystem recovery. Journal of Geology 110, 227–246.

DiMichele, W.A., Mamay, S.H., Chaney, D.S., Hook, R.W., Nelson, W.J., 2001. An Early Permian flora with Late Permian and Mesozoic affinities from north-central Texas. Journal of Paleontology 75, 449–460.

Dimichele, W.A., Kerp, H., Tabor, N.J., Looy, C.V., 2008. The so-called "Paleophytic–Mesophytic" transition in equatorial Pangea — multiple biomes and vegetational tracking of climate change through time. Palaeogeography Palaeoclimatology Palaeoecology 268, 151–163.

Dobruskina, I.A., 1980. Stratigraphic Position of Plant-bearing Beds of the Triassic of Eurasia (Stratigraficheskoe polozhenie floronosnikh tolsch triasa Evrazii). Nauka, Moscow. 161 pp.

Dworkin, S.I., Nordt, L., Atchley, S., 2005. Determining terrestrial paleotemperature using the oxygen isotopic composition of pedogenic carbonate. Earth and Planetary Science Letters 237, 56–68.

Ekart, D.D., Cerling, T.E., Montañez, I.P., Tabor, N.J., 1999. A 400 million year isotope record of pedogenic carbonate; implications for paleoatmospheric carbon dioxide. American Journal of Science 299, 805–827.

Engoren, M., Retallack, G.J., 2004. Vertebrate extinction across the Permian–Triassic boundary in the Karoo Basin of South Africa: comment and reply. Geological Society of America Bulletin 116, 1295–1296.

Etter, W., 2002. *Grès a Voltzia*: preservation in early Mesozoic deltaic and marginal marine environments. In: Bottjer, D.J., Etter, W., Hagadorn, J.W., Tang, C.M. (Eds.), Exceptional Fossil Preservation: A Unique View of the Evolution of Marine Life. Columbia University Press, New York, pp. 205–220.

Fielding, C.R., Frank, T.D., Lauren, P., Birgenheier, L.P., Rygel, M.C., Jones, A.T., Roberts, J., 2008. Stratigraphic imprint of the Late Paleozoic Ice Age in eastern Australia: a record of alternating glacial and nonglacial climate regime. Geological Society London Journal 165, 129–140.

Freeman, K.H., Pagani, M., 2005. Alkenone-based estimates of past CO_2 levels: a consideration of their utility based on an analysis of uncertainties. In: Ehleringer, J.R., Cerling, T.E., Dearing, M.D. (Eds.), A History of Atmospheric CO_2 and its Effect on Plants, Animals, and Ecosystems. Springer, Berlin, pp. 35–61.

Fröbisch, J., 2008. Global taxonomic diversity of anomodonts (Tetrapoda, Therapsida) and the terrestrial rock record across the Permian–Triassic boundary. PloS One 3 (e3733), 1–14.

Gand, G., Garric, J., Schneider, J., Sciau, J., Walter, H., 1996. Biocoenoses à méduses du Permien français (Basin de Saint-Affrique, Massif Central). Geobios 29, 379–400.

Gastaldo, R.A., Adendorff, R., Bamford, M., Labandeira, C.C., Neveling, J., Sims, H., 2005. Taphonomic trends of macrofloral assemblages across the Permian–Triassic boundary, Karoo Basin, South Africa. Palaios 20, 479–497.

Gastaldo, R.A., Neveling, J., Vlarke, C.K., Newbury, S.S., 2009. The terrestrial Permian–Triassic boundary event bed is a nonevent. Geology 37, 199–202.

Gradstein, F., Ogg, J., Smith, A., 2004. A Geologic Time Scale 2004. Cambridge University Press, Cambridge. 588 pp.

Grasby, S.E., Sanei, H., Beauchamp, B., 2011. Catastrophic dispersion of coal fly ash into oceans during the latest Permian extinction. Nature Geoscience 4, 104–107.

Grice, K., Vao, C.-Q., Love, G.D., Böttcher, M.E., Twitchett, R.J., Grosjean, E., Summons, R.E., Turgeon, S.C., Dunning, W., Jin, Y.-G., 2005. Photic zone euxinia during the Permian–Triassic superanoxic event. Science 307, 706–709.
Grimaldi, D., Engel, M.S., 2005. Evolution of the Insects. Cambridge University Press, Cambridge. 755 pp.
Groenewald, G.H., 1991. Burrow casts from the *Lystrosaurus–Procolophon* zone. Koedoe 34, 13–22.
Gulbranson, E.L., Montañez, I.P., Tabor, N.J., 2011. A proxy for humidity and floral province from paleosols. Journal of Geology 119, 559–573.
Hankel, O., 1992. Late Permian to Early Triassic microfloral assemblages from Maji ya Chumvi, Kenya. Review of Palaeobotany and Palynology 72, 129–147.
Henderson, C.M., 2005. International correlation of the marine Permian time scale. In: Lucas, S.G., Ziegler, K.E. (Eds.), The non-marine Permian: New Mexico Museum of Natural History and Science Bulletin, 30, pp. 104–105.
Heydari, E., Hassandzadeh, J., 2003. Deev Jahi model of the Permian–Triassic boundary mass extinction: a case for gas hydrates as the main cause of the biological crisis on Earth. Sedimentary Geology 163, 147–163.
Huey, R.B., Ward, P.D., 2005. Hypoxia, global warming, and terrestrial Late Permian extinctions. Science 308, 398–401.
Hussakof, L., 1916. Note on a palaeoniscid fish from a Permian formation in South Dakota. American Journal of Science 6, 347–350.
Inosemtsev, S.A., Targulian, V.O., 2010. Verkhmepermskie paleopochvi: svoistva, proshessi, usloviya formirovaniya (Upper Permian Paleosols: Features, Processes, Environment). Geos, Moscow. 186 pp.
Joachimski, M.M., Lai, X., Shen, S., Jiang, H., Luo, G., Chen, B., Chen, J., Sun, Y., 2012. Climate warming in the latest Permian and the Permian–Triassic mass extinction. Geology 40, 195–198.
Johnson, S.C., Lucas, S.G., Hunt, A.P., 2002. Macro-fish fauna of the upper Triassic (Apachean) Redonda Formation, eastern New Mexico. In: Lucas, S.G. (Ed.), Upper Triassic stratigraphy and paleontology of New Mexico: New Mexico Museum of Natural History and Science Bulletin, 21, pp. 107–113.
Johnson, C.L., Amory, J.A., Zinniker, D., Lamb, M.A., Graham, S.A., Altoffer, M., Badarch, G., 2008. Sedimentary response to arc–continent collision, Permian, southern Mongolia. In: Draut, A., Clift, P.D., Scholl, D.W. (Eds.), Formation and applications of the sedimentary record in arc collision zones: Geological Society of America Special Paper, 436, pp. 363–390.
Kaufman, A.J., Xiao, S., 2003. High CO_2 levels in the Proterozoic atmosphere estimated from analyses of individual microfossils. Nature 425, 279–282.
Kazarinova, V.P., 1979. Kori vivetraniya sibiri (Siberian Crusts of Weathering). Nedra, Moscow. v.2, 249 pp.
Kearsey, T., Twitchett, R.J., Newell, A.J., 2012. Origin and significance of pedogenic dolomite from the South Urals of Russia. Geological Magazine 149, 291–307.
Kitching, J.W., Raath, M.A., 1984. Fossils from the Elliot and Clarens Formation (Karoo sequence) of the northeastern Cape, Orange Free State and Lesotho, and a suggested biozonation based on tetrapods. Palaeontologia Africana 25, 111–125.
Korte, C., Kozur, H.W., 2010. Carbon isotope stratigraphy across the Permian–Triassic boundary: a review. Journal of Asian Earth Sciences 39, 215–235.
Korte, C., Pande, P., Kozur, H.W., Joachimski, M.M., Oberhänsli, H., 2010. Massive volcanism at the Permian–Triassic boundary and its impact on the isotopic composition of the ocean and atmosphere. Journal of Asian Earth Sciences 37, 293–311.
Kozur, H.W., Weems, R.E., 2011. Detailed correlation and age of continental late Changhsingian and earliest Triassic beds: implications for the role of the Siberian Trap in the Permian–Triassic biotic crisis. Palaeogeography Palaeoclimatology Palaeoecology 308, 22–40.
Krassilov, V., Karasev, E., 2009. Paleofloristic evidence of climate change near and beyond the Permian–Triassic boundary. Palaeogeography Palaeoclimatology Palaeoecology 284, 326–336.
Krull, E.S., Retallack, G.J., 2000. $\delta^{13}C_{org}$ depth profiles from paleosols across the Permian–Triassic boundary: evidence for methane release. Geological Society of America Bulletin 112, 1459–1472.
Kubo, T., Benton, M.J., 2009. Tetrapod postural shift estimated from Permian and Triassic trackways. Palaeontology 52, 1029–1037.
Kump, L.R., Pavlov, A., Arthur, M.A., 2005. Massive eruption of hydrogen sulfide to the surface ocean and atmosphere during intervals of oceanic anoxia. Geology 33, 397–400.
Lai, S., Qin, J., Li, Y., Li, S., Santosh, M., 2012. Permian high Ti/Y basalts from the eastern part of the Emeishan Large Igneous Province, southwestern China: petrogenesis and tectonic implications. Journal of Asian Earth Sciences 47, 216–230.
Lindström, S., McLoughlin, S., 2007. Synchronous palynofloristic extinction and recovery after the end-Permian event in the Prince Charles Mountains, Antarctica: implications for palynofloristic turnover across Gondwana. Review of Palaeobotany and Palynology 145, 89–122.
Lucas, S.G., 2006. Global Permian tetrapod biostratigraphy and biochronology. In: Lucas, S.G., Cassinis, G., Schneider, J. (Eds.), Non-marine Permian biostratigraphy and biochronology: Geological Society London Special Publication, 265, pp. 65–93.
Lucas, S.G., 2009. Timing and magnitude of tetrapod extinctions across the Permo–Triassic boundary. Journal of Asian Earth Sciences 36, 491–502.
Lüthi, D., Le Floch, M., Bereiter, B., Blunier, T., Barnola, J.-M., Siegenthaler, U., Raynaud, D., Jouzel, J., Fischer, H., Kawamura, K., Stocker, T.F., 2008. High-resolution carbon dioxide concentration record 650,000–800,000 years before Present. Nature 453, 379–382.
MacRae, C., 1999. Life Etched in Stone: Fossils of South Africa. Geological Survey of South Africa, Johannesburg. 305 pp.
Maynard, J.B., 1992. Chemistry of modern soils as a guide to interpreting Precambrian paleosols. Journal of Geology 100, 279–289.
McFadden, L.D., Tinsley, J.C., 1985. Rate and depth of pedogenic-carbonate accumulation in soils: formulation and testing of a compartment model. In: Weide, D.L. (Ed.), Soils and Quaternary geology of the southwestern United States: Geological Society of America Special Paper., 203, pp. 23–41.
Metcalfe, I., Nicoll, R.S., Willink, R.J., 2008. Conodonts from the Permian–Triassic transition in Australia and position of the Permian–Triassic boundary. Australian Journal of Earth Sciences 55, 365–377.
Metcalfe, I., Foster, C.B., Afonin, S.A., Nicoll, R.S., Mundil, R., Wang, X.-F., Lucas, S.G., 2009. Stratigraphy, biostratigraphy and C isotopes of the Permian–Triassic non-marine sequence at Dalongkou and Lucaogou, Xinjiang province, China. Asian Earth Sciences Journal 36, 503–520.
Meyen, S.V., 1982. The Carboniferous and Permian Floras of Angaraland (A Synthesis). International, Lucknow. 110 pp.
Milner, A.R., 1981. On the identity of "*Ptyonius bendai*" (Amphibia) from the Lower Permian of Kost'alov, Czechoslovakia. Neues Jahrbuch für Geologie und Paläontologie 6, 346–352.
Mogutcheva, N.K., Krugovykh, V.V., 2009. New data on the stratigraphic chart for Triassic deposits in the Tunguska Syneclise and Kuznetsk Basin. Stratigraphy and Geological Correlation 17, 510–518.
Mogutcheva, N.K., Naugolnykh, S.V., 2010. *Gagariostropbis cylindricus* (Prynada) Mogutcheva and the Permian–Triassic ecosystem flora reorganization in the Tunguska Basin. Stratigraphy and Geological Correlation 18, 31–41.
Montañez, I.P., Tabor, N.J., Niemeier, D., DiMichele, W.A., Frank, T.D., Fielding, C.R., Isbell, J.L., Birgenheier, L.P., Rygel, M.C., 2007. CO_2-forced climate and vegetation instability during Late Paleozoic deglaciation. Science 315, 87–91.
Morante, R., 1996. Permian and early Triassic isotopic records of carbon and strontium in Australia and a scenario of events about the Permian–Triassic boundary. Historical Biology 11, 289–310.
Naugolnykh, S.V., Mogutcheva, N.K., 2006. Novii predstaviteli plaunovidnikh (Lycopidiopsida) iz nizhnego Triasa Tungusska Syneclisi (Sibirskaya Platforma) [A new representative of *Isoetes* (Lycopodiopsida) from the Lower Triassic of the Tunguksa Basin (Siberian Platform)]. Geologiya i Geofiziki 47, 81–93.
Newell, A.J., Benton, M.J., Kearsey, T., Taylor, G.K., Twitchett, R.J., Tverdokhelbov, V.P., 2012. Calcretes, fluviolacustrine sediments and subsidence patterns in Permo–Triassic salt-walled minibasins of the south Urals. Russia, Sedimentology. Online 22 Feb 2012. doi:10.1111/j.1365-3091.01390.x.
Olsen, P.E., Johansson, A.K., 1994. Field guide to Late Triassic tetrapod sites in Virginia and North Carolina. In: Fraser, N.C., Sues, H.-D. (Eds.), In the Shadow of the Dinosaurs: Early Mesozoic Tetrapods. Cambridge University Press, Cambridge, pp. 409–430.
Ovtcharova, M., Bucher, H., Schaltegger, U., Galfetti, T., Brayard, A., Guex, J., 2006. New Early to Middle Triassic U–Pb ages from South China: calibration with ammonoid biozones and implications for the timing of the Triassic biotic recovery. Earth and Planetary Science Letters 243, 463–475.
Pearson, P.N., Palmer, M.R., 1999. Middle Eocene seawater pH and atmospheric carbon dioxide concentrations. Science 284, 1824–1826.
Prochnow, S.J., Nordt, L.C., Atchley, S.C., Hudec, M.R., 2006. Multi-proxy paleosol evidence for middle and late Triassic climate trends in eastern Utah. Palaeogeography Palaeoclimatology Palaeoecology 232, 53–72.
Retallack, G.J., 1995. Permian–Triassic life crisis on land. Science 267, 77–80.
Retallack, G.J., 1996. Early Triassic therapsid footprints from the Sydney Basin, Australia. Alcheringa 20, 301–314.
Retallack, G.J., 1997a. A Colour Guide to Paleosols. John Wiley and Sons, Chichester. 175 pp.
Retallack, G.J., 1997b. Palaeosols in the upper Narrabeen Group of New South Wales as evidence of Early Triassic palaeoenvironments without exact modern analogues. Australian Journal of Earth Sciences 44, 185–201.
Retallack, G.J., 1997c. Earliest Triassic origin of *Isoetes* and quillwort evolutionary radiation. Journal of Paleontology 71, 500–521.
Retallack, G.J., 1999. Post-apocalyptic greenhouse paleoclimate revealed by earliest Triassic paleosols in the Sydney Basin, Australia. Geological Society of America Bulletin 111, 52–70.
Retallack, G.J., 2001. Soils of the Past, Second edition. Blackwell, Oxford. 600 pp.
Retallack, G.J., 2002. Carbon dioxide and climate over the past 300 million years. In: Gröcke, D.R., Kucera, M. (Eds.), Understanding climate change: proxies, chronology and ocean–atmosphere interactions: Philosophical Transactions of the Royal Society of London Series A, 360, pp. 659–674.
Retallack, G.J., 2005a. Pedogenic carbonate proxies for amount and seasonality of precipitation in paleosols. Geology 33, 333–336.
Retallack, G.J., 2005b. Permian greenhouse crises. In: Lucas, S.G., Zeigler, K.E. (Eds.), The nonmarine Permian: New Mexico Museum of Natural History and Science Bulletin, 30, pp. 256–269.
Retallack, G.J., 2009a. Greenhouse crises of the past 300 million years. Geological Society of America Bulletin 121, 1441–1455.
Retallack, G.J., 2009b. Refining a pedogenic CO_2 paleobarometer for quantifying the middle Miocene greenhouse spike. Palaeogeography Palaeoclimatology Palaeoecology 281, 57–65.
Retallack, G.J., 2011. Exceptional fossil preservation during CO_2 greenhouse crises? Palaeogeography Palaeoclimatology Palaeoecology 307, 59–74.
Retallack, G.J., Hammer, W.R., 1998. Paleoenvironment of the Triassic therapsid *Lystrosaurus* in the central Transantarctic Mountains, Antarctica. Antarctic Journal of the United States 31 (2), 33–35.
Retallack, G.J., Huang, C.-M., 2011. Ecology and evolution of Devonian trees in New York, USA. Palaeogeography Palaeoclimatology Palaeoecology 299, 110–128.
Retallack, G.J., Jahren, A.H., 2008. Methane outbursts from igneous intrusion of coal at the Permian–Triassic boundary. Journal of Geology 116, 1–20.
Retallack, G.J., Krull, E.S., 1999. Landscape ecological shift at the Permian–Triassic boundary in Antarctica. Australian Journal of Earth Sciences 46, 786–812.

Retallack, G.J., Veevers, J.J., Morante, R., 1996. Global early Triassic coal gap between Late Permian extinction and Middle Triassic recovery of peat-forming plants. Bulletin of the Geological Society of America 108, 195–207.
Retallack, G.J., Smith, R.M.H., Ward, P.D., 2003. Vertebrate extinction across the Permian–Triassic boundary in the Karoo Basin, South Africa. Geological Society of America Bulletin 115, 1133–1152.
Retallack, G.J., Jahren, A.H., Sheldon, N.D., Chakrabarti, R., Metzger, C.A., Smith, R.M.H., 2005. The Permian–Triassic boundary in Antarctica. Antarctic Science 17, 241–258.
Retallack, G.J., Metzger, C.A., Greaver, T., Jahren, A.H., Smith, R.M.H., Sheldon, N.D., 2006. Middle–Late Permian mass extinction on land. Geological Society of America Bulletin 118, 1398–1411.
Retallack, G.J., Greaver, T., Jahren, A.H., 2007. Return to Coalsack Bluff and the Permian–Triassic boundary in Antarctica. Global and Planetary Change 55, 90–108.
Retallack, G.J., Sheldon, N.D., Carr, P.F., Fanning, M., Thompson, C.A., Williams, M.L., Jones, B.G., Hutton, A., 2011. Multiple Early Triassic greenhouse crises impeded recovery from Late Permian mass extinction. Palaeogeography Palaeoclimatology Palaeoecology 308, 233–251.
Rothman, D.H., 2002. Atmospheric carbon dioxide levels for the last 500 million years. Proceedings of the National Academy of Sciences of the United States of America 99, 4167–4171.
Royer, D.L., 2006. CO_2-forced climate thresholds during the Phanerozoic. Geochimica et Cosmochimica Acta 70, 5665–5675.
Royer, D.L., Berner, R.A., Beerling, D.J., 2001. Phanerozoic atmospheric CO_2 change: evaluating geochemical and paleobiological approaches. Earth-Science Reviews 54, 349–392.
Royer, D.L., Berner, R.A., Park, J., 2007. Climate sensitivity constrained by CO_2 concentrations over the past 420 million years. Nature 446, 530–532.
Rubidge, B.S., 1995. Biostratigraphy of the Beaufort Group (Karoo Supergroup). South African Committee for Stratigraphy Biostratigraphy Series, 1. 45 pp.
Ryskin, G., 2003. Methane-driven oceanic eruptions and mass extinction. Geology 31, 741–744.
Sadovnikov, G.N., 2008. On the global stratotype section and point of the Triassic base. Lithology and Geological Correlation 16, 31–46.
Sadovnikov, G.N., 2011. Triasovaya flora Taimira (Triassic Flora of Taimyr). Gosudarstvennii Darbinovskii Muzei, Moscow. 156 pp.
Sadovnikov, G.N., Orlova, E.F., 1990. Vozrast kontinelatl'nykh vulkanogennykh otlozheny severa sredney sibiri (Age of continental volcanogenic deposits of northern Arctic Siberia). Izvestiya Akademii Nauk S.S.R. Seriya Geologicheskaya 3, 58–70.
Sanei, H., Grasby, S.E., Beauchamp, B., 2012. Latest Permian mercury anomalies. Geology 40, 63–66.
Sarkar, A., Yoshioka, H., Ebihara, M., Naraoka, H., 2003. Geochemical and organic carbon isotope studies across the continental Permo–Triassic boundary of Raniganj Basin, eastern India. Palaeogeography Palaeoclimatology Palaeoecology 191, 1–14.
Şengör, A.M.C., Atayman, S., 2009. The Permian Extinction and the Tethys: an exercise in global geology. Geological Society of America Special Paper, 448. 85 pp.
Sheldon, N.D., 2006. Precambrian paleosols and atmospheric CO_2 levels. Precambrian Research 147, 148–155.
Sheldon, N.D., Retallack, G.J., 2001. Equation for compaction of paleosols due to burial. Geology 29, 247–250.
Sheldon, N.D., Retallack, G.J., 2002. Low oxygen levels in earliest Triassic soils. Geology 30, 919–922.
Sheldon, N.D., Tabor, N.J., 2009. Quantitative paleoenvironmental and paleoclimatic reconstruction using paleosols. Earth-Science Reviews 95, 1–52.
Sheldon, N.D., Retallack, G.J., Tanaka, S., 2002. Geochemical climofunctions from North American soils and application to paleosols across the Eocene–Oligocene boundary in Oregon. Journal of Geology 110, 687–696.
Shen, S.Z., Henderson, C.M., Bowring, S.A., Cao, C.Q., Wang, Y., Wang, W., Zhang, H., Zhang, Y.C., Mu, L., 2010. High-resolution Lopingian (Late Permian) timescale of South China. Geological Journal 45, 122–134.
Shen, S.-Z., Crowley, J.L., Wang, Y., Bowring, S.A., Erwin, D.E., Peter, M., Sadler, P.E., Cao, C.-Q., Rothman, D.H., Henderson, C.M., Ramezani, J., Zhang, H., Shen, Y., Wang, X.-D., Wang, W., Mu, L., Li, W.-Z., Tang, Y.-G., Liu, X.-L., Liu, L.J., Zeng, Y., Jiang, Y.-F., Jin, Y.-G., 2011. Calibrating the end-Permian mass extinction. Science 334, 1367–1372.
Shi, G.R., Waterhouse, J.B., McLoughlin, S., 2010. The Lopingian of Australasia: a review of biostratigraphy, correlations, palaeogeography and palaeobiogeography. Geological Journal 45, 230–265.
Shishkin, M.A., 1998. *Tungussogyrinus* — a relict neotenic dissorophoid (Amphibia, Temnospondyli) from the Permo–Triassic of Siberia. Paleontological Journal 32 (5), 85–96.
Shishkin, M.A., Ochev, V.G., Lozovskii, V.R., Novikov, I.V., 2000. Tetrapod biostratigraphy of the Triassic of Eastern Europe. In: Benton, M.J., Shishkin, M.A., Unwin, D.M., Kurochkin, E.N. (Eds.), The Age of Dinosaurs in Russia and Mongolia. Cambridge University Press, Cambridge, pp. 120–139.
Sidor, C., Miller, M.F., Isbell, J.L., 2008. Tetrapod burrows from the Triassic of Antarctica. Journal of Vertebrate Paleontology 28, 277–284.
Smith, R.M.H., 1987. Helical burrow casts of therapsid origin from the Beaufort Group (Permian) of South Africa. Palaeogeography Palaeoclimatology Palaeoecology 60, 155–170.
Sobolev, S.V., Sobolev, A.V., Kuzmin, D.V., Krivolutskaya, N.A., Petrunin, A.G., Arndt, N.T., Radko, V.A., Vasilev, Y.R., 2011. Linking mantle plumes, large igneous provinces and environmental catastrophes. Nature 477, 312–316.
Solomon, S., Qin, D., Manning, M., Chen, Z., Marquis, M., Averyt, K.B., Tignor, M., Miller, H.L. (Eds.), 2007. Climate Change 2007: The Physical Science Basis. Cambridge University Press, Cambridge. 996 pp.
Szurlies, M., 2007. Latest Permian to Middle Triassic cyclo-magnetostratigraphy from the central European Basin, Germany: implications for the geomagnetic polarity timescale. Earth and Planetary Science Letters 261, 602–619.
Tabor, N.J., 2007. Permo–Pennsylvanian palaeotemperatures from Fe-oxide and phyllosilicate $\delta^{18}O$ values. Earth and Planetary Science Letters 253, 159–171.
Tabor, N.J., Montañez, I.P., 2004. Morphology and distribution of fossil soils in the Permo–Pennsylvanian Wichita and Bowie Groups, north-central Texas, USA: implications for western equatorial Pangean palaeoclimate during icehouse–greenhouse transition. Sedimentology 51, 851–884.
Tabor, N.J., Yapp, C.J., 2005. Juxtaposed Permian and Pleistocene isotopic archives: surficial environments recorded in calcite and goethite from the Wichita Mountains, Oklahoma. Geological Society of America Special Paper 395, 55–70.
Tabor, N.J., Montañez, I.P., Southard, R.L., 2002. Paleoenvironmental reconstruction from chemical and isotopic compositions of Permo–Pennsylvanian pedogenic minerals. Geochimica et Cosmochimica Acta 66, 3093–3107.
Tabor, N.J., Montañez, I.P., Steiner, M.B., Schwindt, D., 2007. $\delta^{13}C$ values of carbonate nodules across the Permian–Triassic boundary in the Karoo Supergroup (South Africa) reflect a stinking sulfurous swamp, not atmospheric CO_2. Palaeogeography Palaeoclimatology Palaeoecology 252, 370–381.
Tabor, N.J., Smith, R.M.H., Steyer, J.S., Sidor, C.A., Poulsen, C.J., 2011. The Permian Moradi Formation of northern Niger: paleosol morphology, petrography and mineralogy. Palaeogeography Palaeoclimatology Palaeoecology 299, 200–213.
Tans, P., Keeling, R., 2011. Recent Mauna Loa CO_2 on NOAA/ESRL website www.esrl.noaa.gov/gmd/ccgg/trends/ (accessed December 30, 2011).
Taylor, G.K., Tucker, C., Twitchett, R.J., Kearsey, T., Benton, M.J., Newell, A., Surkov, M.V., Tverdokhlebov, V.P., 2009. Magnetostratigraphy of Permian/Triassic boundary sequences in the Cis-Urals, Russia: no evidence for a major temporal hiatus. Earth and Planetary Science Letters 281, 36–47.
Thomas, S.G., Tabor, N.J., Yang, W., 2007. Evaluation of pedogenic calcite nodules from the Jiuyucuan Fm, NW China: implications for earliest Triassic pCO_2. Geological Society of America Abstracts 39 (6), 497.
Thomas, S.G., Tabor, N.J., Yang, W., Myers, T.S., Yang, Y., Wang, D., 2011. Palaeosol stratigraphy across the Permian–Triassic boundary, Bogda Mountains, NW China: implications for palaeoenvironmental transition through Earth's largest mass extinction. Palaeogeography Palaeoclimatology Palaeoecology 308, 31–46.
Vörding, B., Kerp, H., 2008. Stomatal indices of *Peltaspermum martinsii* (Pteridospermopsida, Peltaspermaceae) from the upper Permian Bletterbach Gorge and their possible applicability as CO_2 proxies. Neues Jahrbuch für Geologie und Paläontologie Abhandlungen 248, 245–255.
Wade, R.T., 1935. Triassic Fishes of Brookvale. British Museum Natural History, London. 89 pp.
Wang, Z.-Q., 1996. Recovery of vegetation from the terminal Permian mass extinction in North China. Review of Palaeobotany and Palynology 91, 121–142.
Ward, P.D., Montgomery, D.R., Smith, R., 2000. Altered river morphology in South Africa related to the Permian–Triassic extinction. Science 289, 1740–1743.
Ward, P.D., Botha, J., Buick, R., de Kock, M.O., Erwin, D.H., Garrison, G., Kirschvink, J., Smith, R., 2005. Abrupt and gradual extinction among Late Permian vertebrates in the Karoo Basin. Science 307, 609–610.
Wignall, P.B., Sun, Y.-D., Bond, D.P.G., Izon, G., Newton, R.J., Vedrine, S., Widdowson, M., Ali, J.R., Lai, L., Jiang, H.S., Cope, H., Bottrell, S.H., 2009. Volcanism, mass extinction and carbon isotope fluctuations in the Permian of China. Science 324, 1179–1182.
Witzmann, F., Pfritzschner, H.D., 2003. Larval ontogeny of *Micromelerpeton credneri* (Temnospondyli: Dissorophoidea). Journal of Vertebrate Paleontology 23, 750–768.
Woodward, A.S., 1890. The fossil fishes of the Hawkesbury Series at Gosford. Geological Survey of New South Wales Palaeontology Memoir, 4. 32 pp.
Woodward, A.S., 1908. The fossil fishes of the Hawkesbury Series at St Peters. Geological Survey of New South Wales Palaeontology Memoir, 10. 55 pp.
Wright, R.P., Askin, R.A., 1987. The Permian–Triassic boundary in the southern Morondava Basin of Madagascar as defined by plant microfossils. In: McKenzie, G.D. (Ed.), Gondwana six: stratigraphy, sedimentology and paleontology: American Geophysical Union Geophysical Monograph, 42, pp. 157–166.
Wynn, J.G., 2003. Towards a physically based model of CO_2-induced stomatal frequency response. New Phytologist 157, 391–398.
Wynn, J.G., 2007. Carbon isotope fractionation during decomposition of organic matter in soils and paleosols; implications for paleoecological interpretations of paleosols. Palaeogeography Palaeoclimatology Palaeoecology 251, 437–448.
Xiong, C., Wang, Q., 2011. Permian–Triassic land–plant diversity in South China: was there a mass extinction at the Permian/Triassic boundary? Paleobiology 37, 157–167.
Zhang, F.-F., Xu, H.-F., Konishi, H., Shelobolina, E.S., Roden, E.E., 2012. Polysaccharide-catalyzed nucleation and growth of disordered dolomite — a potential precursor to sedimentary dolomite. American Mineralogist 97, 556–567.

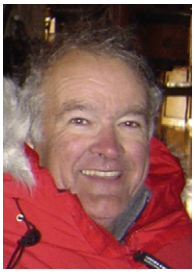

Gregory J. Retallack has been a Professor at the University of Oregon since 1992. Born and raised in Australia, he obtained a BA from Macquarie University in 1973, and a PhD from the University of New England in 1978. His early research and a postdoc at Indiana University (1978–1981) were to study Mesozoic paleobotany. In Eugene, Oregon, since 1981 his research has focused on paleosols as records of major events in the history of life.